Electromagnetic pion form factor at finite temperature

Joel S. Rozowsky

Submitted in partial fulfilment of the requirements
for the degree of Master of Science
at the
UNIVERSITY OF CAPE TOWN

September 2, 1994

Abstract

The electromagnetic form factor of the pion in the space-like region, and at finite temperature, $F_\pi(Q^2, T)$, is obtained from a Finite Energy QCD Sum Rule. The form factor decreases with increasing T, and vanishes at some critical temperature, where the pion radius diverges, thus signalling quark deconfinement.

Contents

Chapter 1

Introduction

1.1 QCD

In the early 1930's the theory of quantum electrodynamics (QED) was developed to describe the interactions of electrons and photons. QED is the most successful Quantum Field Theory, as it has been used to make very precise predictions of electromagnetic observables using a method of theoretical perturbative approximations.

Quantum Chromodynamics (QCD) has emerged in the last few decades as the only description of the strong interaction without any manifest defects. However, unlike QED, QCD is a non-abelian gauge theory. It describes the dynamics of quarks and gluons in terms of a local gauge theory based on the colour symmetry group $SU(3)_c$.

Quarks come in a variety of flavours (up, down, strange, charm, bottom (or beauty) and top (or truth)) and each can have one of three colours (red, green and blue). Each has a baryon number $\frac{1}{3}$ and an electric charge of magnitude either $\frac{1}{3}$ or $\frac{2}{3}$. Further, to ensure that the baryons and mesons have spins $\frac{1}{2}$ and 1 respectively, the quarks are required to have spin $\frac{1}{2}$. The success of this representation was first realized when Gell-Mann [1] showed that extending the $SU(2)$ isospin symmetry, between the proton and neutron, to the flavour symmetry $SU(3)_f$ (i.e. of the light quarks), then some of the representations of the symmetry group exactly fitted the quantum number structure of the observed

hadrons. This led to the prediction of the as yet unobserved Ω^- in the spin $\frac{3}{2}$ decuplet before it was discovered at Brookhaven in 1963. All hadron states (baryons and mesons) are colour singlets, i.e. physical states are invariant under transformations of the group $SU(3)_c$.

Now analogously to the photon in QED which mediates the interaction of the charged particles, the gluon in QCD is the non-abelian gauge field that mediates the colour interactions between quarks. As there is one photon which is the gauge boson corresponding to the generator of the abelian gauge group $U(1)$ in QED, there are eight gluons in QCD which correspond to each of the generators of the group $SU(3)_c$ (i.e. $3^2 - 1$).

However, due to the complete failure to observe free quarks subsequent to Gell-Mann's revelations, the physics community was somewhat skeptical about the physical existence of quarks (they were regarded as useful mathematical entities with no physical reality). Several experimental results now give evidence for the existence of quarks and gluons. They are

- In the e^+e^- annihilation experiment with very high energy e^+e^- collisions, one expects that the ratios of the cross-sections $\sigma(e^+e^- \rightarrow \text{hadrons})$ and $\sigma(e^+e^- \rightarrow \mu^+\mu^-)$ should be

$$R = \frac{\sigma(e^+e^- \rightarrow \text{hadrons})}{\sigma(e^+e^- \rightarrow \mu^+\mu^-)} = N_c \sum_{q=1}^{N_f} e_q^2 \tag{1.1}$$

  from theoretical predictions [2]. In eq.(1.1) N_c is the number of colours and N_f is the number of flavours. One would expect that as the energy increases one would pass the thresholds for $s\bar{s}$, $c\bar{c}$ and $b\bar{b}$ production (the existence of the top quark has yet to be confirmed) and so the sum on the right hand side of eq.(1.1) should yield the correct values of the ratio in the different energy regions. If one looks at a plot of R against $\sqrt{s}$ (center of mass energy) we see that for $\sqrt{s} < 3$ GeV then $R = 2$, for $4 < \sqrt{s} < 9$ GeV then $R = \frac{10}{3}$ and for $\sqrt{s} > 10$ GeV then $R = \frac{11}{3}$, which correspond to the values of R for $N_f = 3, 4, 5$ respectively as

$$\begin{aligned} R = \; & 3\left[\left(\tfrac{2}{3}\right)^2 + \left(\tfrac{1}{3}\right)^2 + \left(\tfrac{1}{3}\right)^2\right] = 2 && \text{for u,d,s} \\ = \; & 2 + 3\left(\tfrac{2}{3}\right)^2 = \tfrac{10}{3} && \text{for u,d,s,c} \\ = \; & \tfrac{10}{3} + 3\left(\tfrac{1}{3}\right)^2 = \tfrac{11}{3} && \text{for u,d,s,c,b} \end{aligned} \tag{1.2}$$

- For the process $\pi^0 \rightarrow 2\gamma$ the decay rate can be predicted using the lowest order Feynman diagram.

$$\Gamma(\pi^0 \rightarrow 2\gamma) = N_c^2(q_u^2 - q_d^2)^2 \frac{\alpha^2 m_{\pi^0}^2}{64\pi^3 f_\pi^2} \tag{1.3}$$

  The observed width is $\Gamma(\pi^0 \rightarrow 2\gamma) = 7.95 \pm 0.55$ eV which is in excellent agreement with $N_c = 3$ [3].

- Deep inelastic scattering experiments (leptons off hadrons) have been conducted at CERN and SLAC [4]. These experiments show that the constituents of the hadrons are point-like. The neutrino data [4] shows that the difference between the number of quarks and anti-quarks in a nucleon is 2.81 ± 0.16 which is consistent with having 3 valance quarks in a nucleon. It was also shown using the Adler sum rule that the difference between the number of u and d quarks in a proton was 1.07 ± 0.20. And finally, from the muon and neutrino scattering, the charges of the u and d quarks were measured to be 0.64 ± 0.05 and 0.41 ± 0.09 respectively (i.e. consistent with charges of $\frac{2}{3}$ and $\frac{1}{3}$).

- 3-jet e^+e^- events have been observed at PETRA [5] and are consistent with the existence of gluons with spin-parity 1^-.

Initially the perturbative approach which was successful for QED, was thought not possible for QCD due to the fact that the coupling constant $g^2/4\pi$ was calculated to be greater than unity. However, in 1973 it was shown by Politzer [6] and Gross & Wilczek [7] that the 'running coupling constant' α_s is not constant and depends on the separation distance. At short distances (high energies) α_s is quite small and a perturbative approach is viable, however at large distances (low energies) α_s is large. This phenomenon is known as *Asymptotic Freedom*. Perturbative QCD is accurate at high energies but at low energies (for e.g. the hadron spectrum) one needs non-perturbative effects like vacuum condensates.

1.2 QCD sum rules

In the last decade a great deal of effort has been made towards finding reliable methods for performing calculations in the non-perturbative region of QCD. These efforts have been divided into two main categories: 'brute force' computational techniques (eg. Lattice QCD calculations) and analytical calculations.

The approach of QCD sum rules was introduced by Shifman, Vainshtein and Zakharov (SVZ) in 1979 [8]. They did not try to solve the problem of confinement, but rather they assumed that confinement existed and included it into the theory through the use of a few parameters. These parameters are the so called condensates and thus allow one to obtain many hadronic properties though appropriate sum rules.

One starts by considering a two-point function

$$\Pi(q) = i \int d^4x \, e^{iqx} < 0|T\{J(x)J^\dagger(0)\}|0 > \tag{1.4}$$

with a current $J(x)$ composed of the quark and gluon fields entering into the QCD Lagrangian. Wilson proposed a short distance operator product expansion (OPE) in [9] of the following form

$$A(x)B(0) \sim \sum_r C_r(x)\mathcal{O}_r(0) \tag{1.5}$$

where A and B are two local operators. If one sandwiches this expansion between initial and final vacuum states then the two-point function in eq.(1.4) can be written as

$$\Pi(q^2) = C_I + \sum_r C_r(q^2) < 0|\mathcal{O}_r|0 > \tag{1.6}$$

where the Wilson coefficients in this expansion (the $C_r(q^2)$'s) depend on the Lorentz indices and quantum numbers of the current $J(x)$ and also of the local gauge invariant operators $\mathcal{O}_r$. The operators $\mathcal{O}_r$ are built from the quark and gluon fields. The operator C_I is calculated from purely perturbative QCD. In the OPE in eq.(1.6) one assumes that the short and long distance effects factorize (i.e. that the short distance effects are used in constructing the Wilson coefficients and that the long distance effects are buried in

the vacuum condensates $< 0|\mathcal{O}_r|0 >$). Now on analytical grounds the two-point function must satisfy a dispersion relation (this can be proved using Cauchy's theorem), i.e. that

$$\Pi(Q^2) = \frac{1}{\pi}\int_0^\infty ds \frac{Im\Pi(s)}{s+Q^2} + \text{ subtraction terms} \tag{1.7}$$

where $Q^2 = -q^2$. Then spectral sum rules are constructed and one relates the hadronic spectral function to that one from the OPE. Different kinds of sum rules can be constructed by taking Hilbert, Laplace and Gaussian transforms of the dispersion equation (eq.(1.7)). Different type of sum rules are appropriate for different types of applications.

Chapter 2

Electromagnetic pion form factor at $T = 0$

2.1 Introduction

QCD Sum Rules as proposed by Shifman, Vainshtein and Zakharov [8] have successfully been used to determine the masses of the low-lying resonances. This work, continued by [10, 11] and others, was successful in determining the masses of the lowest-lying meson and baryon resonances in practically all conceivable channels in terms of only a few QCD parameters (e.g. that of Λ_{QCD}, the quark mass m_q, the gluon $< 0|G^a_{\mu\nu}G^a_{\mu\nu}|0 >$ and quark $< 0|q\bar{q}|0 >$ vacuum condensates). This work was extended by them to the problem next in complexity, the determination of the dynamic characteristics of the resonances. One of which is the electromagnetic form factors. The electromagnetic pion form factor at $T = 0$ has been extensively studied using Finite Energy QCD Sum Rules (FESR), as well as with Laplace transform QCD Sum Rules by Ioffe and Smilga [12], Nesterenko and Radyushkin [13], and Eletsky and Kogan [14] (it has also been studied using an Extended Operator Product Expansion (EOPE) by Chetyrkin *et al.* in [15, 16]). This can be done by considering the three-point function in the Euclidean region for a suitably chosen quark current.

2.2 The method

Consider the three-point function :-

$$\Pi_{\mu\nu\lambda}(p,p',q) = i^2 \int d^4x\, d^4y\, e^{i(p'x-qy)} < 0|T\{j^{\dagger}_{A\nu}(x), j^{el}_{\lambda}(y), j_{A\mu}(0)\}|0 >, \qquad (2.1)$$

where $j_{A\mu}(x)$ is the axial-vector light quark current given by $j_{A\mu}(x) = \overline{u}(x)\gamma_\mu\gamma_5 d(x)$, $j^{el}_{\lambda}(x)$ is the electromagnetic current, and $q = p' - p$ is the momentum transfer.

On general analyticity grounds, the three-point function eq.(2.1) can be written as (where $Q^2 = -q^2$),

$$\Pi_{\mu\nu\lambda}(p,p',Q^2) = \frac{1}{\pi^2}\int_0^\infty ds \int_0^\infty ds' \, \frac{\rho_{\mu\nu\lambda}(s,s',Q^2)}{(s+p^2)(s'+p'^2)} \; + \text{ subtraction terms.} \qquad (2.2)$$

satisfying the double dispersion relation. The subtraction terms can be eliminated either by taking Laplace/Borel transforms or by considering a finite energy QCD sum rule. Now the QCD sum rule program can be summarized as follows. The left hand side of eq.(2.2) in the Euclidean region can be calculated in QCD through the Operator Product Expansion (OPE), to any desired order in perturbation theory, parameterizing non-perturbative effects in terms of vacuum expectation values of the same quark and gluon fields entering the QCD Lagrangian. Contact with the hadronic world is made by writing the spectral function appearing in the double dispersion relation on the right-hand side of eq.(2.2) in terms of all possible hadronic states contributing to the three-point function. Normally a reasonable saturation of the dispersion relation is achieved by considering the ground state, followed after some threshold energy S_0 by a hadronic continuum modeled by perturbative QCD, i.e.

$$\begin{aligned}
\rho_{\mu\nu\lambda}(s,s',Q^2)|_{HAD} &= < 0|j_{A\nu}(0)|\pi^+(p') >< \pi^+(p')|j^{el}_{\lambda}(0)|\pi^+(p) > \\
&\quad \times < \pi^+(p)|j_{A\mu}(0)|0 > \delta(s)\delta(s') \; + \; \text{continuum}, \qquad (2.3) \\
&= 2f_\pi^2 F_\pi(Q^2) p'_\nu p_\mu (p_\lambda + p'_\lambda)\delta(s)\delta(s') \\
&\quad + \; \rho_{\mu\nu\lambda}(s,s',Q^2)|_{QCD}\,[1 - \theta(S_0 - s - s')]\,. \qquad (2.4)
\end{aligned}$$

where $f_\pi \simeq 93$ MeV, $F_\pi(Q^2)$ is the electromagnetic form factor and in our approximation of massless quarks (i.e. the chiral limit) we put $m_\pi^2 = 0$. As discussed before we leave out the explicit contributions of higher states including the A_1 meson (however the A_1 meson is implicitly included in the continuum), however these could in principle be included in the hadronic spectral function eq. (2.3).

2.3 Calculation of the lowest order loop diagram

We can calculate the leading order contribution to the correlator $\Pi_{\mu\nu\lambda}$ by considering the lowest order Feynman diagram (figure 2.1). There will be contributions due to higher

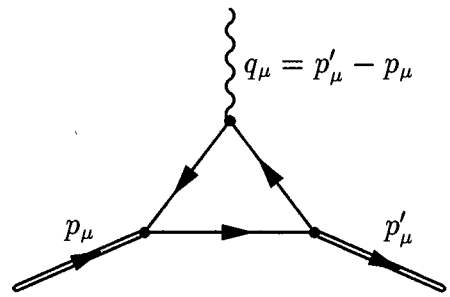

Figure 2.1: Lowest order loop diagram contributing to the three-point function $\Pi_{\mu\nu\lambda}$.

order perturbative corrections (an example of one second-order loop diagram contributing to $\Pi_{\mu\nu\lambda}$ can be seen in figure 2.2), however in the virtuality region of interest ($|p|^2 \simeq |p'|^2 \simeq |q|^2 \simeq 1$ GeV^2) perturbative corrections will be small, $\alpha_s/\pi \sim 0.1$ (where α_s is the QCD 'running coupling constant') and thus will be neglected.

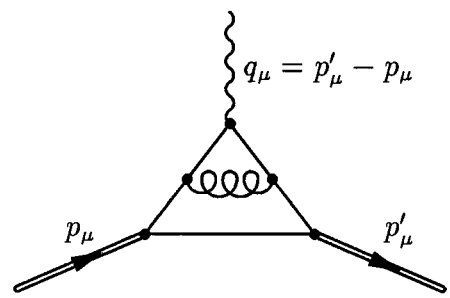

Figure 2.2: Example of a higher order loop diagram contributing to the three-point function $\Pi_{\mu\nu\lambda}$.

Now by using straight-forward Feynman rules we can get an integral expression for the lowest order graph (figure 2.1),

$$\Pi^{(0)}_{\mu\nu\lambda}(p,p',q) = \frac{i}{(2\pi)^4}\int \frac{d^4k\, Tr\{\gamma_\nu\gamma_5 \not{k}\gamma_\mu\gamma_5(\not{p}-\not{k})\gamma_\lambda(\not{p}'-\not{k})\}}{k^2(p'-k)^2(p-k)^2}$$
$$= \frac{-i}{(2\pi)^4} Tr\{\gamma_\nu\gamma_\alpha\gamma_\mu\gamma_\beta\gamma_\lambda\gamma_\sigma\}\int \frac{d^4k\, k^\alpha(p^\beta-k^\beta)(p'^\sigma-k^\sigma)}{k^2(p'-k)^2(p-k)^2} \qquad (2.5)$$

Thus by using a standard recursive technique with the basic anti-commutation relationships of the γ_μ matrices (eq.(2.6)) one can easily determine an expression for the trace in eq.(2.5).

$$\gamma^\mu\gamma^\nu + \gamma^\nu\gamma^\mu = 2g^{\mu\nu} \qquad (2.6)$$

$$T^{\nu\alpha\mu\beta} \equiv Tr\{\gamma^\nu\gamma^\alpha\gamma^\mu\gamma^\beta\} = 4\{g^{\nu\alpha}g^{\mu\beta} - g^{\nu\mu}g^{\alpha\beta} + g^{\nu\beta}g^{\alpha\mu}\} \qquad (2.7)$$

then

$$Tr\{\gamma^\nu\gamma^\alpha\gamma^\mu\gamma^\beta\gamma^\lambda\gamma^\sigma\} = \{g^{\lambda\sigma}T^{\nu\alpha\beta\mu} - g^{\beta\sigma}T^{\nu\alpha\mu\lambda} + g^{\mu\sigma}T^{\nu\alpha\beta\lambda}$$
$$- g^{\alpha\sigma}T^{\nu\mu\beta\lambda} + g^{\nu\sigma}T^{\alpha\mu\beta\lambda}\} \qquad (2.8)$$

We can obtain the spectral function $\rho^{(0)}_{\mu\nu\lambda}(s,s',Q^2)$ corresponding to the correlator (see eq.(2.2)) by putting the quark lines in the graph of figure 2.1 on-mass-shell and substituting the denominators of the quark propagators by δ-functions according to Cutkosky's rule, $1/k^2 \to -2\pi i\delta(k^2)$. Once we have done this we obtain an expression which is comprised of the following integrals (note since we have assumed that the light quarks are massless, we have neglected the mass of the pion),

$$I = \int d^4k\, \delta(k^2)\delta[(p-k)^2]\delta[(p'-k)^2] \qquad (2.9)$$

$$I_\mu = \int d^4k\, k_\mu\delta(k^2)\delta[(p-k)^2]\delta[(p'-k)^2] \qquad (2.10)$$

$$I_{\mu\nu} = \int d^4k\, k_\mu k_\nu\delta(k^2)\delta[(p-k)^2]\delta[(p'-k)^2] \qquad (2.11)$$

$$I_{\mu\nu\lambda} = \int d^4k\, k_\mu k_\nu k_\lambda\delta(k^2)\delta[(p-k)^2]\delta[(p'-k)^2] \qquad (2.12)$$

In order to calculate I, eq.(2.9)[1], we consider a convenient reference frame. Once eq.(2.9) is solved in a particular frame the expression will be generalized to a Lorentz invariant

[1]We will later see that the other integrals, equations (2.10),(2.11) ,(2.12), can be computed using a standard recursive technique and the solution to I, eq.(2.9).

expression. So for convenience we chose the frame where the 3-momentum of p_μ and p'_μ are parallel, ie $\vec{p} \parallel \vec{p}'$. Then the three δ-functions in eq. (2.9) can be expanded as follows,

$$\delta[k^2] = \frac{1}{2|\vec{k}|}\left\{\delta[k_0 - |\vec{k}|] + \delta[k_0 + |\vec{k}|]\right\} \tag{2.13}$$

$$\delta[(p-k)^2] = \delta[p^2 - 2(k_0 p_0 - |\vec{k}||\vec{p}|\cos\theta)] \tag{2.14}$$

$$\delta[(p'-k)^2] = \delta[p'^2 - 2(k_0 p'_0 + |\vec{k}||\vec{p}'|\cos\theta)] \tag{2.15}$$

In equations (2.13),(2.14),(2.15) $p_\mu = (p_0, \vec{p})$, $p'_\mu = (p'_0, \vec{p}')$, $k_\mu = (k_0, \vec{k})$ and θ is the angle between $\vec{p}$ and $\vec{k}$. Then by rewriting equations (2.14) and (2.15) as δ-functions of the variables $\cos\theta$ and k_0 respectively, the integral reduces to the following form,

$$\begin{aligned} I &= \frac{\pi}{4\,|p'_0|\vec{p}| + p_0|\vec{p}'||} \int dz \left\{\delta\left[z - \frac{1}{2}\frac{p'^2|\vec{p}| + p^2|\vec{p}'|}{|p'_0|\vec{p}| + p_0|\vec{p}'||}\right]\right. \\ &\quad \left. + \delta\left[z + \frac{1}{2}\frac{p'^2|\vec{p}| + p^2|\vec{p}'|}{|p'_0|\vec{p}| + p_0|\vec{p}'||}\right]\right\} \qquad (2.16) \\ &= \frac{\pi}{4\,|p'_0|\vec{p}| + p_0|\vec{p}'||} \qquad (2.17) \end{aligned}$$

Only one of the δ-functions contribute in eq.(2.16) as $z \equiv |\vec{k}|$, which is a positive quantity. Now the expression in eq. (2.17) can with some careful manipulation be rewritten in terms of the following Lorentz invariant variables: p^2, p'^2, Q^2 ($Q^2 = -q^2$). So then

$$I = \frac{\pi}{2\lambda^{1/2}} \tag{2.18}$$

where,

$$\lambda(s, s', Q^2) = (s + s' + Q^2)^2 - 4ss' \tag{2.19}$$

Now as described in [17] the other integrals, equations (2.10),(2.11),(2.12) can be calculated using a recursive technique. I will describe how it can be done for eq. (2.10). Let

$$\begin{aligned} I_\mu &= \int d^4k\, k_\mu \delta(k^2)\delta[(p-k)^2]\delta[(p'-k)^2] \\ &= A(p,p')p_\mu + B(p,p')p'_\mu \qquad (2.20) \end{aligned}$$

I_μ can only have the structures p_μ and p'_μ (remember $q_\mu = p'_\mu - p_\mu$). Thus by considering the two contractions $p^\mu I_\mu$ and $p'^\mu I_\mu$ we get two simultaneous linear equations in A and B. Solving for A and B yields,

$$A(p,p') = \frac{(p.p')p'^\mu - p'^2 p^\mu}{(p.p')^2 - p^2 p'^2} I_\mu \tag{2.21}$$

$$B(p,p') = \frac{(p.p')p^\mu - p^2 p'^\mu}{(p.p')^2 - p^2 p'^2} I_\mu \tag{2.22}$$

So to solve for A and B all one needs is the integrals $p^\mu I_\mu$ and $p'^\mu I_\mu$, which using the δ-functions in the integrals each reduces to a factor times I, eq.(2.9). Reincorporating these back into eq.(2.20) gives the solution to eq.(2.10) that,

$$I_\mu = -\frac{\pi}{2\lambda^{3/2}} \left[s'(s - s' - Q^2)p_\mu + s(s' - s - Q^2)p'_\mu \right] \tag{2.23}$$

thus similarly $I_{\mu\nu}$ (eq.(2.11)) can be solved by writing $I_{\mu\nu}$ as a combination of the following Lorentz structures: $g_{\mu\nu}$, $p_\mu p_\nu$, $p'_\mu p'_\nu$ and $p_\mu p'_\nu$.

The spectral function $\rho_{\mu\nu\lambda}(s,s',Q^2)$ is equal to the double discontinuity of the amplitude of $\Pi_{\mu\nu\lambda}$ divided by $(2\pi i)^2 = -4\pi^2$. Thus after some calculations using the explicit solutions to the integrals in equations (2.9),(2.10), (2.11),(2.12) we obtain the following expression,

$$\begin{aligned}
\rho^{(0)}_{\mu\nu\lambda}(s,s',Q^2) = \frac{3}{8\pi^2}\frac{Q^2}{\lambda^{5/2}} \Big\{ & \Big[\frac{10x}{\lambda} Q^2 (x+Q^2)^3 - (x+Q^2)(4x^2 + 11xQ^2 + Q^4) \\
& + \lambda(2x+Q^2) \Big] \tfrac{1}{2} P_\lambda (p_\mu p_\nu + p'_\mu p'_\nu) - \tfrac{1}{2} P_\lambda (p_\mu p_\nu - p'_\mu p'_\nu) y \\
& \times \Big[\frac{10}{\lambda} Q^2 (x+Q^2)^3 - 3(x+3Q^2)(x+Q^2) + \lambda \Big] + P_\lambda (x+Q^2)^2 p'_\nu p_\mu \\
& \times \Big[2x + 5Q^2 - \frac{5Q^2}{\lambda}(x+Q^2)^2 \Big] + P_\lambda p_\nu p'_\mu (x^2 - y^2) \Big[2x + 3Q^2 \\
& - \frac{5Q^2}{\lambda}(x+Q^2)^2 \Big] + \tfrac{1}{2} q_\lambda (p_\mu p_\nu + p'_\mu p'_\nu) y \frac{1}{Q^2} \\
& \times \Big[-Q^4(x+Q^2) - \lambda Q^2 - x \Big(\frac{10}{\lambda} Q^2 (x+Q^2)^3 - (2x+7Q^2)(x+Q^2) + 2\lambda \Big) \Big] \\
& - \tfrac{1}{2} q_\lambda (p_\mu p_\nu - p'_\mu p'_\nu) \frac{1}{Q^2} \Big[- Q^4 x (x+Q^2) - \lambda Q^2 x \\
& - y^2 \Big(\frac{10}{\lambda} Q^2 (x+Q^2)^3 - 2x - 7Q^2 + 2\lambda \Big) \Big] - q_\lambda p'_\nu p_\mu y \frac{x+Q^2}{Q^2} \\
& \times \Big[(x+4Q^2)(x+Q^2) - \lambda - \frac{5Q^2}{\lambda}(x+Q^2)^3 \Big]
\end{aligned}$$

$$
\begin{aligned}
&-p_\nu p'_\mu q_\lambda y(x^2-y^2)\frac{1}{Q^2}\left[(x+2Q^2-\frac{5Q^2}{\lambda}(x+Q^2)^2\right] \\
&-\tfrac{1}{2}\delta_{\mu\nu}P_\lambda(x^2-y^2)\left[\lambda-Q^2(x+Q^2)\right]+\tfrac{1}{2}\delta_{\mu\nu}q_\lambda\frac{1}{Q^2}(x^2-y^2) \\
&\times\left[\lambda-Q^2(x+Q^2)\right]+\tfrac{1}{2}(\delta_{\mu\lambda}p_\nu+\delta_{\nu\lambda}p'_\mu)(x^2-y^2)\left[\lambda+Q^2(x+Q^2)\right] \\
&+\tfrac{1}{2}(\delta_{\mu\lambda}p_\nu-\delta_{\nu\lambda}p'_\mu)y(x^2-y^2)(x+Q^2) \\
&-\tfrac{1}{2}(\delta_{\nu\lambda}p_\mu+\delta_{\mu\lambda}p'_\nu)(x+Q^2)\left[\lambda(2x+Q^2)-Q^2(x+Q^2)^2\right] \\
&+\tfrac{1}{2}(\delta_{\nu\lambda}p_\mu-\delta_{\mu\lambda}p'_\nu)y(x+Q^2)\left[\lambda+(x+Q^2)^2\right]\Big\}. \qquad (2.24)
\end{aligned}
$$

where $P=p+p'$, $q=p'-p$, $x=s+s'$ and $y=s-s'$. This expression for the spectral function eq.(2.24) includes 14 different tensor structures. However not all these tensors structures are independent as the spectral function obeys the following tranversality conditions.

$$p^\mu\rho_{\mu\nu\lambda}(s,s',Q^2)=p'^\nu\rho_{\mu\nu\lambda}(s,s',Q^2)=q^\lambda\rho_{\mu\nu\lambda}(s,s',Q^2)=0 \qquad (2.25)$$

2.4 Constructing the QCD sum rule for the pion form factor

We have an expression for the spectral function as described by the hadronic world, eq.(2.4), and we have a similar expression calculated in QCD for the first order loop-diagram, eq.(2.24). So in order to construct the QCD sum rule we first write eq.(2.4) in terms of P_μ and q_μ instead of p_μ and p'_μ. Then

$$f_\pi^2F_\pi(Q^2)p_\mu p'_\nu P_\lambda=\tfrac{1}{4}f_\pi^2F_\pi(Q^2)\left[P_\mu P_\nu P_\lambda+P_\lambda(P_\mu q_\nu-P_\nu q_\mu)-q_\mu q_\nu P_\lambda\right] \qquad (2.26)$$

So to find the electromagnetic pion form factor we shall write the sum rule for the coefficients of the most symmetric looking tensor structure $P_\mu P_\nu P_\lambda$ (in theory the sum rule could be constructed by considering any of the tensor structures). Now by again replacing p_μ and p'_μ by P_μ and q_μ in eq.(2.24), we can extract the coefficient of $P_\mu P_\nu P_\lambda$ for the QCD

spectral density.

$$\rho^{(0)}(s,s',Q^2)|_{QCD} = \frac{3Q^4}{16\pi^2\lambda^{7/2}}\left[3\lambda(x+Q^2)(x+2Q^2) - \lambda^2 - 5Q^2(x+Q^2)^3\right] \qquad (2.27)$$

We are going to consider the lowest moment finite energy QCD sum rule for F_π, which is equivalent to taking the double Borel transform of the double dispersion relation relation, eq.(2.2), and then setting $M^2 \to \infty$ (M^2 is the parameter introduced by considering a Borel transform, see Appendix A). By doing this one does not have to calculate the vacuum condensates, as they enter the sum rule as inverse powers of M^2 and thus their contribution goes to zero in the limit $M^2 \to \infty$.

Thus we can construct the sum rule by equating the hadronic sector described in eq.'s (2.4),(2.26) to that of the quark (QCD) sector described in eq.(2.27).

$$\tfrac{1}{2}f_\pi^2 F_\pi(Q^2)\int_\Omega \delta(s)\delta(s')\,dsds' = \int_\Omega dsds'\,\rho^{(0)}(s,s',Q^2)|_{QCD} \qquad (2.28)$$

Where Ω is a region of integration in the s, s' plane defined by the θ-function in eq.(2.4). The region Ω is the region of integration left over when the integration over the QCD continuum on the left hand side of eq.(2.28) cancels with the equivalent region on the right hand side. Solving for $F_\pi(Q^2)$ gives the following

$$F_\pi(Q^2) = \frac{2}{f_\pi^2}\int_\Omega dsds'\,\rho^{(0)}(s,s',Q^2)|_{QCD} \qquad (2.29)$$

Now the region of integration Ω is a triangle in the s, s' plane (see figure 2.3). However the shape of the integration region does not affect the result much (if one uses a square region (see figure 2.3) instead, i.e. re-writing the θ-function in eq.(2.4) as $\theta(S_1 - s)\theta(S_1 - s')$, then the resultant $F_\pi(Q^2)$ does not vary more than 20% from the 'triangle' version). Thus by using the 'triangle' region one can transform the double integral over s and s' into a double integral over x and y (where x and y are defined as before in section 2.3).

$$F_\pi(Q^2) = \frac{1}{f_\pi^2}\int_0^{S_0} dx \int_{-x}^{x} dy\rho(x,y,Q^2)|_{QCD} \qquad (2.30)$$

In this form the integral in y can be calculated readily yielding

$$F_\pi(Q^2) = \frac{1}{4\pi^2 f_\pi^2}\int_0^{S_0} x^2\frac{(2x+3Q^2)}{(2x+Q^2)^3}dx \qquad (2.31)$$

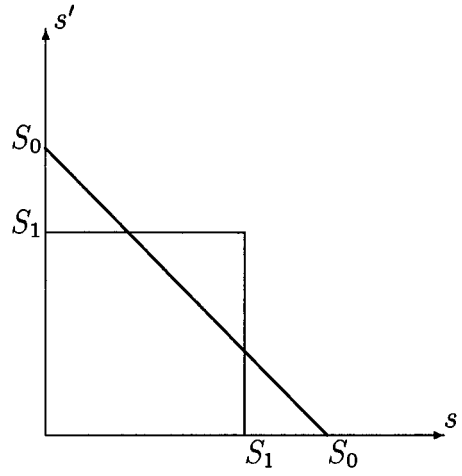

Figure 2.3: Here we can see two possible integration regions in the s, s' plane ($S_0 = \sqrt{2}S_1$ for equal areas).

and integrating over x gives (as in [13])

$$F_\pi(Q^2) = \frac{S_0}{16\pi^2 f_\pi^2} \frac{1}{(1 + Q^2/2S_0)^2} \tag{2.32}$$

In eq.(2.32) $S_0 \simeq 1$ GeV^2, and $f_\pi \simeq 93$ MeV. It is not however, evident in eq.(2.32) that this is only valid for $Q^2 \geq 1$ GeV^2, where one expects a reasonable convergence of the OPE (terms in the OPE come in as inverse powers of Q^2). In figure 2.4 we can see the behavior of F_π against Q^2. If one compares this to experimental data [18] then one gets a reasonable fit for $Q^2 \simeq 1 - 4$ GeV^2. This limitation is of little relevancy as we will later investigate the behavior of $F_\pi(Q^2, T)/F_\pi(Q^2, 0)$ along this Q^2 interval.

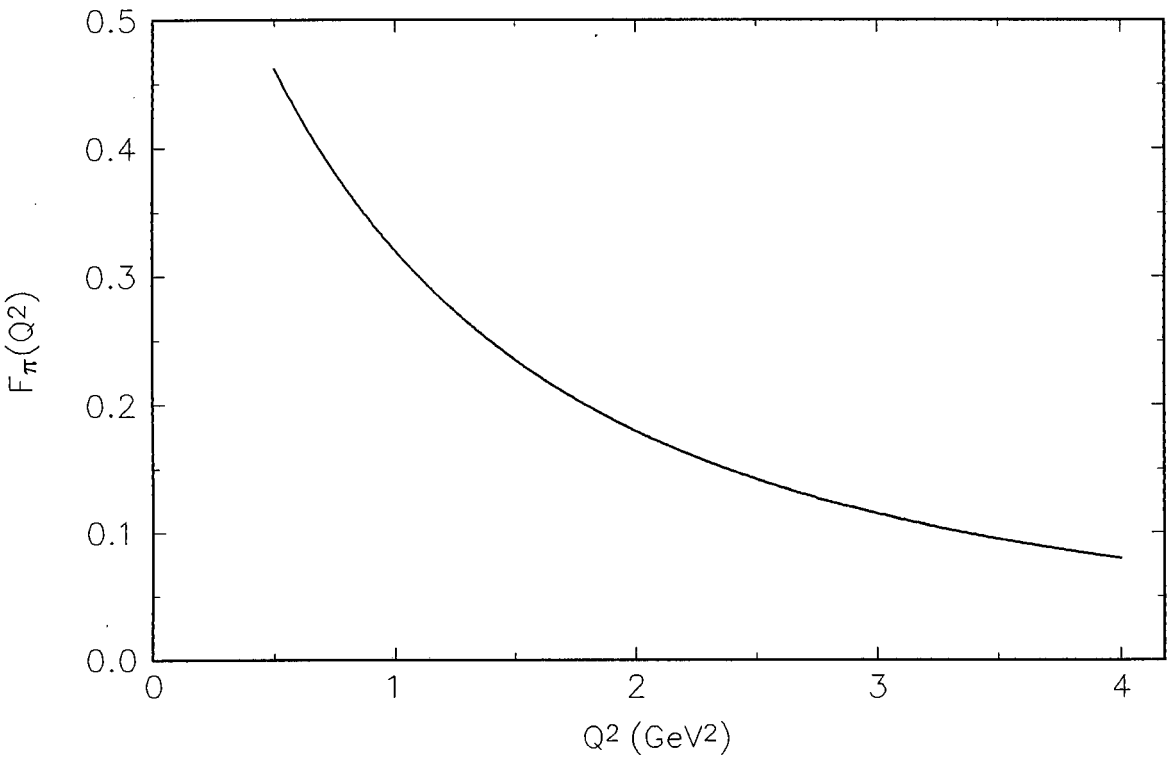

Figure 2.4: The electromagnetic pion form factor $F_\pi(Q^2)$ against Q^2 (in GeV^2) at $T = 0$ from eq.(2.32).

Chapter 3

Temperature dependent QCD sum rules

3.1 Finite temperature propagators

In order to do finite temperature QCD calculations one should know the behaviour of the quark and gluon propagators for finite temperature. Dolan and Jackiw developed a formalism [19] where they derived finite temperature versions of the spinless Bose and Fermion propagators.

When considering a finite temperature field theory the Green's function is defined by

$$G_\beta(x_1,\ldots,x_j) = \frac{Tr\left\{e^{-\beta H}T(\varphi(x_1)\cdots\varphi(x_j))\right\}}{Tr\{e^{-\beta H}\}} \tag{3.1}$$

where $\varphi(x)$ is the field corresponding to the Hamiltonian H. β is inversely proportional to the temperature ($\beta = 1/k_B T$).

3.1.1 Spinless Bose fields

Using the definition of eq.(3.1), the finite-temperature 2-point function can be written as

$$\begin{aligned} D_\beta(x-y) &= \frac{Tr\left\{e^{-\beta H}T(\varphi(x)\varphi(y))\right\}}{Tr\{e^{-\beta H}\}} \\ &= \langle T(\varphi(x)\varphi(y))\rangle \end{aligned} \tag{3.2}$$

which for non-interacting fields satisfies

$$(\Box_x + m^2)D_\beta(x-y) = -\delta^4(x-y) \tag{3.3}$$

Boundary conditions must be specified in order to solve this equation. In order to derive a real time representation for $D_\beta(x-y)$ we will first derive an imaginary time representation of the Green's function. The time arguments of D_β are continued to the interval $0 \leq ix_0, iy_0 \leq \beta$, and we define the time ordering by imaginary time, then

$$\langle T(\varphi(x)\varphi(y))\rangle = \begin{cases} <\varphi(x)\varphi(y)> \equiv D_\beta^>(x-y) & ix_0 > iy_0 \\ <\varphi(y)\varphi(x)> \equiv D_\beta^<(x-y) & iy_0 > ix_0 \end{cases} \tag{3.4}$$

and therefore

$$\begin{aligned} D_\beta(x-y)|_{x_0=0} &= D_\beta^<(x-y)|_{x_0=0} \\ D_\beta(x-y)|_{x_0=-i\beta} &= D_\beta^>(x-y)|_{x_0=-i\beta} \end{aligned} \tag{3.5}$$

then if we consider

$$\begin{aligned} (Tre^{-\beta H})D_\beta^<(x-y)|_{x_0=0} &= Tr\left\{e^{-\beta H}\varphi(y_0,\vec{y})\varphi(0,\vec{x})\right\} \\ &= Tr\left\{e^{-\beta H}e^{\beta H}\varphi(0,\vec{x})e^{-\beta H}\varphi(y_0,\vec{y})\right\} \\ &= Tr\left\{e^{-\beta H}\varphi(-i\beta,\vec{x})\varphi(y_0,\vec{y})\right\} \\ &= (Tre^{-\beta H})D_\beta^>(x-y)|_{x_0=-i\beta} \end{aligned} \tag{3.6}$$

Then using this together with eq.(3.2) and eq.(3.5) gives us the desired periodic boundary condition that

$$D_\beta(x-y)|_{x_0=0} = D_\beta(x-y)|_{x_0=-i\beta} \tag{3.7}$$

Since D_β is periodic we can write D_β as a double Fourier series and integral over energy-momentum space.

$$D_\beta(x-y) = \frac{1}{(-i\beta)}\sum_n e^{-i\omega_n x_0}\int\frac{d^3p}{(2\pi)^3}\frac{1}{(-i\beta)}\sum_{n'}e^{i\omega_{n'}y_0}\int\frac{d^3p'}{(2\pi)^3}D_\beta(\omega_n,\vec{p},\omega_{n'},\vec{p}') \quad (3.8)$$

where the indices n, n' run over the set of integers and $\omega_n = \frac{2\pi n}{-i\beta}$. Similarly the inverse formulation is

$$D_\beta(\omega_n,\vec{p},\omega_{n'},\vec{p}') = \int_0^{-i\beta} dx_0\, e^{i\omega_n x_0}\int d^3x\, e^{-\vec{p}.\vec{x}}\int_0^{-i\beta} dy_0\, e^{-i\omega_{n'}y_0}\int d^3y\, e^{\vec{p}'.\vec{y}}D_\beta(x-y) \quad (3.9)$$

The expression in eq.(3.9) can be dramatically simplified since the integrand D_β only depends on the co-ordinate difference. This diagonalizes the transformation.

$$D_\beta(\omega_n,\vec{p},\omega_{n'},\vec{p}') = -i\beta\delta_{nn'}(2\pi)^3\delta^3(\vec{p}-\vec{p}')D_\beta(\omega_n,\vec{p}) \quad (3.10)$$

Using this simplification

$$D_\beta(x-y) = \frac{1}{(-i\beta)}\sum_n e^{-i\omega_n(x_0-y_0)}\int\frac{d^3p}{(2\pi)^3}e^{i\vec{p}.(\vec{x}-\vec{y})}D_\beta(p) \quad (3.11)$$

and

$$D_\beta(p) = \int_0^{-i\beta} dx_0\int d^3x\, e^{ipx}D_\beta(x) \quad (3.12)$$

where $p^\mu = (\omega_n,\vec{p})$. This vector is space-like as $p^2 = \omega_n^2 - \vec{p}^{\,2} = -\left(\frac{4\pi^2n^2}{\beta^2}+\vec{p}^{\,2}\right) \leq 0$. Substituting eq.(3.11) into eq.(3.3) yields the following result.

$$\begin{aligned}
(\Box_x + m^2)D_\beta(x-y) &= (\Box_x+m^2)\frac{1}{(-i\beta)}\sum_n e^{-i\omega_n(x_0-y_0)}\int\frac{d^3p}{(2\pi)^3}e^{i\vec{p}.(\vec{x}-\vec{y})}D_\beta(p)\\
&= \frac{1}{(-i\beta)}\sum_n e^{-i\omega_n(x_0-y_0)}\int\frac{d^3p}{(2\pi)^3}e^{i\vec{p}.(\vec{x}-\vec{y})}(-\omega_n^2+\vec{p}^{\,2}+m^2)D_\beta(p)\\
&= \frac{1}{(-i\beta)}\sum_n e^{-i\omega_n(x_0-y_0)}\int\frac{d^3p}{(2\pi)^3}e^{i\vec{p}.(\vec{x}-\vec{y})}(-p^2+m^2)D_\beta(p)\\
&= -i\delta^4(x-y) \quad (3.13)
\end{aligned}$$

Inverting this expression gives

$$(-p^2+m^2)D_\beta(p) = -i\int_0^{-i\beta} dz_0\int d^3z\,\delta^4(z) \quad (3.14)$$

where $z = x - y$, and thus the Green's function for the imaginary time representation is

$$D_\beta(p) = \frac{i}{p^2 - m^2} \tag{3.15}$$

Then it is possible to obtain the real time representation of $D_\beta(x-y)$ by use of Fourier integrals. First we define the Fourier transform of $D_\beta^{\gtrless}(x)$ by $\overline{D}_\beta^{\gtrless}(k)$ where

$$\overline{D}_\beta^{\gtrless}(k) = \int d^4x\, e^{ikx} D_\beta^{\gtrless}(x) \tag{3.16}$$

Then

$$\begin{aligned}
\overline{D}_\beta^{<}(k) &= \int d^4x\, e^{i(k_0 x_0 - \vec{k}.\vec{x})} D_\beta^{<}(x_0, \vec{x}) \\
&= \int d^4x\, e^{i(k_0 x_0 - \vec{k}.\vec{x})} D_\beta^{>}(x_0 - i\beta, \vec{x}) \\
&= e^{-\beta k_0} \int d^4x\, e^{i(k_0 x_0 - \vec{k}.\vec{x})} D_\beta^{>}(x_0, \vec{x}) \\
&= e^{-\beta k_0} \overline{D}_\beta^{>}(k)
\end{aligned} \tag{3.17}$$

where eq.(3.6) was used in going from the first to the second equality and the integration variable x_0 was redefined in going from the second to the third equality. Now if we define

$$\rho(k) = \overline{D}_\beta^{>}(k) - \overline{D}_\beta^{<}(k) \tag{3.18}$$

and

$$\overline{D}_\beta^{<}(k) = f(k_0)\rho(k) \tag{3.19}$$

then

$$\overline{D}_\beta^{>}(k) = [1 + f(k_0)]\rho(k) \tag{3.20}$$

and using eq.(3.17) together with eq's (3.19) and (3.20) gives

$$f(k_0) = \frac{1}{e^{\beta k_0} - 1} \tag{3.21}$$

which is easily recognizable as the thermal Bose-Einstein distribution. The real time Green's function $\overline{D}_\beta(k)$ can be written as a Fourier integral of $D_\beta(x)$.

$$
\begin{aligned}
\overline{D}_\beta(k) &= \int d^4x\, e^{ikx} D_\beta(x) \\
&= \int d^4x\, e^{ikx} [\theta(x_0) D^>_\beta(x) + \theta(-x_0) D^<_\beta(x)] \\
&= \int d^4x\, e^{ikx} \left[D^>_\beta(x) i \int_{-\infty}^{\infty} \frac{dk'_0}{2\pi} \frac{e^{i(k'_0-k_0)x_0}}{i\epsilon - (k'_0 - k_0)} + D^<_\beta(x) i \int_{-\infty}^{\infty} \frac{dk'_0}{2\pi} \frac{e^{-i(k'_0-k_0)x_0}}{i\epsilon - (k'_0 - k_0)} \right] \\
&= i \int_{-\infty}^{\infty} \frac{dk'_0}{2\pi} \left[\frac{1}{k_0 - k'_0 + i\epsilon} \int d^4x\, e^{i(k'_0 x_0 - \vec{k}.\vec{x})} D^>_\beta(x) \right. \\
&\qquad \left. - \frac{1}{k_0 - k'_0 - i\epsilon} \int d^4x\, e^{i(k'_0 x_0 - \vec{k}.\vec{x})} D^<_\beta(x) \right] \\
&= i \int_{-\infty}^{\infty} \frac{dk'_0}{2\pi} \left[\frac{\overline{D}^>_\beta(k'_0, \vec{k})}{k_0 - k'_0 + i\epsilon} - \frac{\overline{D}^<_\beta(k'_0, \vec{k})}{k_0 - k'_0 - i\epsilon} \right] \\
&= i \int_{-\infty}^{\infty} \frac{dk'_0}{2\pi} \rho(k'_0, \vec{k}) \left[\frac{1 + f(k'_0)}{k_0 - k'_0 + i\epsilon} - \frac{f(k'_0)}{k_0 - k'_0 - i\epsilon} \right] \\
&= i \int_{-\infty}^{\infty} \frac{dk'_0}{2\pi} \frac{\rho(k'_0, \vec{k})}{k_0 - k'_0 + i\epsilon} + 2 \int_{-\infty}^{\infty} \frac{dk'_0}{2\pi} \frac{\rho(k'_0, \vec{k}) f(k'_0) \epsilon}{(k_0 - k'_0)^2 + \epsilon^2} \\
&= i \int_{-\infty}^{\infty} \frac{dk'_0}{2\pi} \frac{\rho(k'_0, \vec{k})}{k_0 - k'_0 + i\epsilon} + f(k_0)\rho(k)
\end{aligned}
\tag{3.22}
$$

where the θ-functions in the second equality are rewritten in integral form for the third equality. Also in going from the third to the fourth equality the integration variable k'_0 in the right hand integral is redefined and the second integral in equality seven is an integral involving a δ-function in the limit $\epsilon \to 0$. Thus knowledge of $\rho(k)$ can be used to obtain the real time representation for $\overline{D}_\beta(k)$.

$$
\begin{aligned}
D_\beta(\omega_n, \vec{k}) &= \int_0^{-i\beta} dx_0\, e^{i\omega_n x_0} \int d^3x\, e^{-i\vec{k}.\vec{x}} D_\beta(x) \\
&= \int_0^{-i\beta} dx_0\, e^{i\omega_n x_0} \int d^3x\, e^{-i\vec{k}.\vec{x}} D^>_\beta(x)
\end{aligned}
\tag{3.23}
$$

as $D_\beta(x-y)|_{y=0} = D^>_\beta(x-y)|_{y=0}$ for $x_0 \in [0, -i\beta]$. Then

$$
\begin{aligned}
D_\beta(\omega_n, \vec{k}) &= \int_0^{-i\beta} dx_0\, e^{i\omega_n x_0} \int_{-\infty}^{\infty} \frac{dk_0}{2\pi} e^{-ik_0 x_0} \overline{D}^>_\beta(k) \\
&= i \int_{-\infty}^{\infty} \frac{dk_0}{2\pi} \frac{e^{\beta(\omega_n - k_0)} - 1}{k_0 - \omega_n} [1 + f(k_0)] \rho(k) \\
&= i \int_{-\infty}^{\infty} \frac{dk_0}{2\pi} \frac{\rho(k_0, \vec{k})}{\omega_n - k_0}
\end{aligned}
\tag{3.24}
$$

Thus to determine $\rho(k)$ we extend $D_\beta(\omega_n, \vec{k})$ to a continuous function $D_\beta(k_0, \vec{k})$ and then

in the limit $\epsilon \to 0$

$$\rho(k) = D_\beta(k_0 + i\epsilon, \vec{k}) - D_\beta(k_0 - i\epsilon, \vec{k}) \tag{3.25}$$

This can readily be confirmed by taking the difference of two $D_\beta(k)$'s in integral form (as per eq.(3.24)) and then letting $\epsilon \to 0$. Using the free-field case where $D_\beta(k)$ is given by eq.(3.15) then

$$\rho(k) = \frac{4\epsilon k_0}{(k^2 - m^2)^2 + 4\epsilon^2 k_0^2} \xrightarrow{\epsilon \to 0} 2\pi\epsilon(k_0)\delta(k^2 - m^2) \tag{3.26}$$

where $\epsilon(k_0)$ is the sign of k_0. This limit can be checked by first confirming that for non-zero values of $(k^2 - m^2)$, $\rho(k) \to 0$ in the limit $\epsilon \to 0$ and secondly that integrating $\rho(k)$ over k_0 yields a finite result in the limit $\epsilon \to 0$ (note the $\epsilon(k_0)$ arises when making a substitution $u = k_0^2 \Longrightarrow \epsilon(k_0)du = 2k_0 dk_0$ as u is a positive quantity).

Hence we can obtain the real time Green's function by substituting $\rho(k)$ into eq.(3.22). Therefore

$$\begin{aligned} \overline{D}_\beta(k) &= i\int_{-\infty}^{\infty} \frac{dk_0'}{2\pi} \frac{2\pi\epsilon(k_0)\delta(k^2 - m^2)}{k_0 - k_0' + i\epsilon} + 2\pi f(k_0)\delta(k^2 - m^2) \\ &= \frac{i}{k^2 - m^2 + i\epsilon'} + \frac{2\pi}{e^{\beta E} - 1}\delta(k^2 - m^2) \end{aligned} \tag{3.27}$$

where

$$E = (\vec{k}^2 + m^2)^{1/2} \tag{3.28}$$

and where the ϵ' in eq.(3.27) is an infinitesimal defined as some factor times the ϵ in eq.(3.22).

3.1.2 Fermion fields

The Fermion field real time propagator is derived in an analogous way to the spinless Bose case, except that the anticommutivity of the Fermion fields must be taken into account. So similarly to before

$$\begin{aligned} S_\beta(x - y) &= \frac{Tr\left\{e^{-\beta H} T(\psi(x)\overline{\psi}(y))\right\}}{Tr\{e^{-\beta H}\}} \\ &= \left\langle T(\psi(x)\overline{\psi}(y))\right\rangle \end{aligned} \tag{3.29}$$

which satisfies the Green's function equation for non-interacting fields

$$(i\ \partial\!\!\!/_x - m)S_\beta(x-y) = i\delta^4(x-y) \tag{3.30}$$

where as before S_β is the imaginary time representation for the Fermion Green's function and $\partial\!\!\!/_x = \gamma_\mu \partial_x^\mu$. The time ordering is defined on the complex time interval $[0, -i\beta]$.

$$\left\langle T(\psi(x)\overline{\psi}(y))\right\rangle = \begin{cases} <\psi(x)\overline{\psi}(y)> \equiv S_\beta^>(x-y) & ix_0 > iy_0 \\ <\psi(y)\overline{\psi}(x)> \equiv S_\beta^<(x-y) & iy_0 > ix_0 \end{cases} \tag{3.31}$$

and

$$\begin{aligned} S_\beta(x-y)|_{x_0=0} &= S_\beta^<(x-y)|_{x_0=0} \\ S_\beta(x-y)|_{x_0=-i\beta} &= S_\beta^>(x-y)|_{x_0=-i\beta} \end{aligned} \tag{3.32}$$

which leads to the following anti-periodic boundary condition

$$S_\beta(x-y)|_{x_0=0} = -S_\beta(x-y)|_{x_0=-i\beta} \tag{3.33}$$

and thus one can express $S_\beta(p)$ as a Fourier transform of $S_\beta(x)$,

$$S_\beta(p) = \int_0^{-i\beta} dx_0 \int d^3x\, e^{ipx} S_\beta(x) \tag{3.34}$$

where

$$p^\mu = (\omega_n, \vec{p}) \qquad , \qquad \omega_n = \frac{(2n+1)\pi}{-i\beta} \tag{3.35}$$

which leads to the imaginary time representation for the Green's function by substituting the Fourier integral of eq.(3.34) into eq.(3.30) and solving for $S_\beta(p)$

$$S_\beta(p) = \frac{i}{\not{p} - m} \tag{3.36}$$

As for the Bose-case $\overline{S}_\beta^<(k_0, \vec{k}) = e^{-\beta k_0}\overline{S}_\beta^>(k_0, \vec{k})$ where the definitions of $\overline{S}_\beta^<(k)$ and $\overline{S}_\beta^>(k)$ are similar to before. Then if we define

$$\rho(k) = \overline{S}_\beta^>(k) - \overline{S}_\beta^<(k) \tag{3.37}$$

and

$$\overline{S}_\beta^<(k) = f(k_0)\rho(k) \tag{3.38}$$

then it follows that

$$\overline{S}_\beta^>(k) = [1 + f(k_0)]\rho(k) \tag{3.39}$$

and

$$f(k_0) = \frac{1}{e^{\beta k_0} + 1}\ , \tag{3.40}$$

where $f(k_0)$ is recognizable as the Fermi-Dirac distribution. Then as before the spectral function $\rho(k)$ can be obtained in terms of the imaginary time Green's function $S_\beta(p)$.

$$\begin{aligned} S_\beta(\omega_n, \vec{k}) &= \int_0^{-i\beta} dx_0\, e^{i\omega_n x_0} \int d^3x\, e^{-i\vec{k}.\vec{x}} S_\beta^>(x) \\ &= i\int_{-\infty}^{\infty} \frac{dk_0}{2\pi} \frac{\rho(k_0, \vec{k})}{\omega_n - k_0} \end{aligned} \tag{3.41}$$

so then

$$\rho(k) = S_\beta(k_0 + i\epsilon, \vec{k}) - S_\beta(k_0 - i\epsilon, \vec{k}) \tag{3.42}$$

and so for non-interacting fields the spectral function is

$$\rho(k) = 2\pi\epsilon(k_0)(\not{k} + m)\delta(k^2 - m^2) \tag{3.43}$$

Thus the temperature dependent real time Fermion propagator for non-interacting fields is

$$\begin{aligned} \overline{S}_\beta(k) &= \int d^4x\, e^{ikx}[\theta(x_0)S_\beta^>(x) - \theta(-x_0)S_\beta^<(x)] \\ &= i\int_{-\infty}^{\infty} \frac{dk_0'}{2\pi} \frac{\rho(k_0', \vec{k})}{k_0 - k_0' + i\epsilon} - f(k_0)\rho(k) \\ &= \frac{i}{\not{k} - m + i\epsilon} - \frac{2\pi(\not{k} + m)}{e^{\beta E} - 1}\delta(k^2 - m^2) \end{aligned} \tag{3.44}$$

3.2 Finite temperature QCD current correlators

An extension of the QCD sum rule program to the finite temperature regime was first proposed by Bochkarev and Shaposhnikov [20]. They used a finite temperature QCD sum rules formalism to consider a two-point function involving the vector current. They were thus able to estimate the temperature dependence of the quark condensate and also analyze the temperature dependent behaviour of the parameters S_0 and m (the continuum threshold S_0 and the meson mass m) in the ρ and φ-meson channels.

This work was continued for the axial-vector channel [21] and the nucleon channel [22] using finite energy QCD sum rules. The results from these calculations indicated a substantial rearrangement of the hadronic spectrum with increasing temperature and hint at the existence of a deconfining phase transition (T_d). This was later confirmed by [23] when a more refined formalism was considered which is valid for temperatures near the phase transition.

QCD sum rules as introduced by [8] are based on the operator product expansion (OPE) of current correlators at short distances. The OPE includes non-perturbative effects which are parameterized in terms of a set of quark and gluon vacuum condensates. The values of these condensates cannot be calculated analytically from first principles (this would be equivalent to solving QCD exactly), however they can be estimated from experimental data from eg. e^+e^- annihilation and τ decays or numerically calculated in lattice QCD. Contact with the hadronic world is made through the notion of QCD-hadron duality. When extending this formalism to finite temperature [20] one assumes that the OPE will continue to be valid with temperature dependent vacuum condensates and that the notion of QCD-hadron duality will remain valid. The validity of the OPE at finite temperature cannot be proved (similarly when $T = 0$), however, other field theory models [24] which are exactly solvable have been used to support the validity of the OPE at $T = 0$. This has been extended to finite temperature in [25].

In the temperature dependent QCD sum rules formalism the basic object to be considered is the retarded Gibbs averaged two-point function (as opposed to the zero temperature

version in eq.(1.4))

$$\Pi(q,T) = i \int d^4x\, e^{iqx} \theta(x_0) << [J(x), J^\dagger(0)] >> \tag{3.45}$$

where the $<< \cdots >>$ is the Gibbs averaging defined by

$$<< A.B >> = \sum_n e^{-E_n/T} < n|A.B|n > / Tr\{e^{-\hat{H}/T}\} \tag{3.46}$$

where $|n>$ is a complete set of eigenstates of the QCD Hamiltonian $\hat{H}$. The set of states $|n>$ can be any complete set of states, eg. the hadronic states , the quark-gluon states etc... The natural choice being the quark-gluon basis, as first proposed by [8]. A convincing argument for this choice is presented by [25] where they argue that it would be quite bizarre for the notion of duality to abruptly lose its meaning for some arbitrarily small finite temperature. They argue that the finite temperature contributions to the QCD and hadron spectral function in the space-like region (only the time-like region enters at $T = 0$) are consistent with the zero-temperature formulations as their contributions vanish as $T \to 0$. Also at small temperatures ($T < T_c$) while the heat-bath consists of hadrons this is not in contradiction with the use of a quark-gluon basis as the quarks in the perturbative part of the OPE enter as loops with arbitrary values of momentum.

Now analogously to eq.(1.6) we can write an operator product expansion for the two-point function

$$\Pi(q,T) = C_I << I >> + \sum_r C_r(q) << \mathcal{O}_r >> \tag{3.47}$$

Where the Wilson coefficients $C_r(q)$ contain the Lorentz tensor structures and quantum numbers of $\Pi(q,T)$ and depend on the local gauge-invariant operators $\mathcal{O}_r$ which are constructed from the quark and gluon fields. We will assume that all the temperature dependence is contained in the $<< \mathcal{O}_r >>$'s. This assumption is consistent with factorization of short and long distance effects in the OPE, provided $|\vec{q}^2| \gg (\Lambda_{QCD}, T)$. The first term in the OPE (the $C_I << I >>$ in eq.(3.47)) contains the purely perturbative part of the QCD calculation.

3.3 Determination of the temperature dependence of $S_0(T)$

Now if one considers the two-point function associated with the axial-vector current [21] with $A_\mu(x) = \bar{u}(x)\gamma_\mu\gamma_5 d(x)$ then as per eq.(3.45)

$$\Pi_{\mu\nu}(p,T) = i\int d^4x\, e^{ipx}\theta(x_0) << [A_\mu(x), A_\nu^\dagger(0)] >> \tag{3.48}$$

with the Gibbs average defined as before. Now with the assumptions of a dilute quark gas and zero chemical potential ($\mu = 0$) there are two distinct processes which contribute to the spectral function. The first of which is where the virtual 'quanta' associated with the current $A_\mu(x)$ will convert into $q\bar{q}$ pairs in the time-like region $p^2 = \omega^2 - \vec{p}^{\,2} \geq 4m_q^2$. Secondly for quanta with space-like momenta $(\omega^2 - \vec{p}^{\,2}) \leq 0$, there will be scattering of the quanta with quarks in the gas. The Feynman diagrams of these two processes can be seen in figures 3.1 and 3.2.

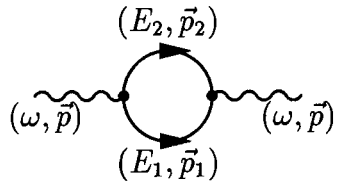

Figure 3.1: Feynman diagram corresponding to the annihilation process for $p^2 \geq 4m_q^2$.

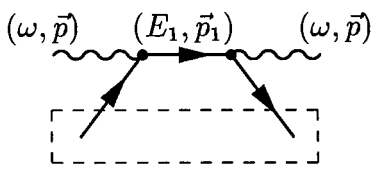

Figure 3.2: Feynman diagram corresponding to the scattering process for $p^2 \leq 0$.

It is important to bear in mind that the so-called 'scattering' process does not imply current scattering off free quarks. Since a loop integration is still implied in figure 3.2,

the term 'scattering' in this context is then misleading. In fact, diagram 3.2 is nothing but diagram 3.1 with the exchange $(E_1, \vec{p}_1) \rightarrow (-E_1, -\vec{p}_1)$. Without thermal corrections to the quark propagators, i.e. at $T = 0$, the spectral functions for both processes are the same (up to a sign). After introducing thermal corrections diagram 3.2 is proportional to T^2, and vanishes at $T = 0$.

The contribution due to the annihilation process (figure 3.1), in the notation of [20] and [21], to the spectral function is as follows

$$\begin{aligned} \frac{1}{\pi} Im\Pi^{(+)}_{\mu\nu}(\omega, \vec{p}) &= \sum_q \int LIPS(\omega, \vec{p}, E_1, \vec{p}_1, E_2, \vec{p}_2) < 0|A_\mu|q\bar{q} >< q\bar{q}|A_\nu|0 > \\ &\quad \times \{[1 - n_F(E_1)][1 - n_F(E_2)] - n_F(E_1)n_F(E_2)\} \end{aligned} \tag{3.49}$$

Also the scattering process (figure 3.2) contributes the following to the spectral function

$$\begin{aligned} \frac{1}{\pi} Im\Pi^{(-)}_{\mu\nu}(\omega, \vec{p}) &= \sum_q \int LIPS(\omega, \vec{p}, -E_1, -\vec{p}_1, E_2, \vec{p}_2) < q|A_\mu|\bar{q} >< \bar{q}|A_\nu|q > \\ &\quad \times \{n_F(E_1)[1 - n_F(E_2)] - n_F(E_2)[1 - n_F(E_1)]\} \end{aligned} \tag{3.50}$$

where

$$LIPS(\omega, \vec{p}, E_1, \vec{p}_1, E_2, \vec{p}_2) = \frac{d^3p_1}{2E_1(2\pi)^3} \frac{d^3p_2}{2E_2(2\pi)^3} \delta(\omega - E_1 - E_2)\delta^3(\vec{p} - \vec{p}_1 - \vec{p}_2) \tag{3.51}$$

indicates the integrals over phase-space. The $n_F(E)$'s in eq's (3.49) and (3.50) are Fermi-Dirac distributions as seen before in eq.(3.40). The two-point function eq.(3.48) can be written in terms of its two tensor structures.

$$\Pi_{\mu\nu}(p, T) = -g_{\mu\nu}\Pi_1(p, T) + p_\mu p_\nu \Pi_0(p, T) \tag{3.52}$$

This is easily verified as the contractions $p^\mu \Pi_{\mu\nu}$ and $p^\nu \Pi_{\mu\nu}$ must vanish. So when one calculates the contribution due to the annihilation term (eq.(3.49)), then this leads to the usual left and right cuts in the complex plane ($\omega \leq -2m_q$ and $\omega \geq 2m_q$ for $\vec{p} = 0$) and does not vanish at $T = 0$. The contribution due to the scattering term leads to a cut centered at $\omega = 0$ and this does vanish at $T = 0$. So concentrating on $\Pi_0(\omega, \vec{p})$ and considering hadron formation at rest with respect to the medium ($\vec{p} \rightarrow 0$), then one

obtains the following

$$\frac{1}{\pi} Im\Pi_0^{(+)}(\omega, \vec{p}=0) = \frac{1}{8\pi^2}\nu(\omega)[3-\nu^2(\omega)]th\left(\frac{\omega}{4T}\right)\theta(\omega^2-4m_q^2) \quad (3.53)$$

$$\frac{1}{\pi} Im\Pi_0^{(-)}(\omega, \vec{p}=0) = \frac{1}{8\pi^2}\delta(\omega^2)\int_{4m_q^2}^{\infty} dz^2\nu(z)[3-\nu^2(z)]2n_F\left(\frac{z}{4T}\right) \quad (3.54)$$

where $\nu(x) = (1-4m_q^2/x^2)^{1/2}$.

On the hadronic side, at low temperatures only pions from the gas will contribute to the spectral function. A good approximation to the hadronic spectral function (neglecting terms of $O(T^4)$) can be made by considering a pion pole plus a continuum modeled by the perturbative QCD expression in eq.(3.53). Then the finite energy QCD sum rule is as follows

$$8\pi^2 f_\pi^2(T) = \tfrac{1}{2}\int_{4m_q^2}^{S_0(T)} dz^2\,\nu(z)[3-\nu^2(z)]th(\frac{z}{4T}) + \int_{4m_q^2}^{\infty} dz^2\,\nu(z)[3-\nu^2(z)]n_F(\frac{z}{2T}) \quad (3.55)$$

where $f_\pi(T)$ is the temperature dependent pion decay constant and $S_0(T)$ is the temperature dependent continuum threshold. Now if we use the low temperature (valid up to order $O(T^2)$) expression for $f_\pi(T)$ as described by Gasser and Leutwyler [26] with

$$f_\pi(T) = \tilde{f}_\pi\left(1 - \frac{N_f}{2\tilde{f}_\pi^2}\frac{1}{(2\pi)^3}\int\frac{d^3p}{E}\left[e^{E/T}-1\right]^{-1}\right) \quad (3.56)$$

where $E^2 = \mu_\pi^2 + p^2$, N_f is the number of quark flavours and $\tilde{f}_\pi = 87$ MeV which is the pion decay constant in the chiral limit (and $T=0$). Then in the chiral limit (ie. $m_q = 0$ and $\nu(z) \to 1$) the FESR in eq.(3.55) becomes (as per [23])

$$8\pi^2 f_\pi^2(T) = \int_0^{S_0(T)} dz^2\,th(\frac{z}{4T}) + 2\int_0^{\infty} dz^2\,n_F(\frac{z}{2T}) \quad (3.57)$$

and substituting for $f_\pi(T)$ from eq.(3.56) gives

$$S_0(T=0) - \frac{10}{3}\pi^2T^2 = \int_0^{S_0(T)} dS\,th(\frac{\sqrt{S}}{4T}) \quad (3.58)$$

where $S_0(T=0) = 8\pi^2\tilde{f}_\pi^2$.

Graphing $S_0(T)/S_0(0)$ and $f_\pi(T)/f_\pi(0)$ show functions decreasing from 1 at $T = 0$ and vanishing at temperatures of about 135 MeV and 250 MeV respectively. The temperature at which $S_0(T)$ vanishes is the critical temperature for deconfinement (T_d), because as the temperature increases the resonances begin to melt and the hadronic spectrum should smooth out and thus $S_0(T)$ is expected to decrease. The temperature at which $f_\pi(T)$ vanishes is the critical temperature for chiral-symmetry restoration (T_c). Now the chiral perturbation theory result from [21] suggests that $T_d < T_c$. However the $f_\pi(T)$ from [26] is only valid at low temperatures. A more refined analysis valid for temperatures close to T_c [23] (ie using a better expression for $f_\pi(T)$) also shows $f_\pi(T)$ and $S_0(T)$ vanishing at temperatures T_c and T_d with T_d only slightly lower than T_c (in [23] the authors remark that either the chiral restoration and deconfinement phase transitions coincide or that they occur at extremely similar temperatures). For our purposes we will assume that T_d and T_c are the same. The analysis of [23] gives the following relationship between $S_0(T)/S_0(0)$ and $f_\pi(T)/f_\pi(0)$

$$\frac{S_0(T)}{S_0(0)} \simeq \frac{f_\pi^2(T)}{f_\pi^2(0)} \tag{3.59}$$

A graph of $S_0(T)/S_0(0)$ and $f_\pi(T)/f_\pi(0)$ can be seen in figure 3.3.

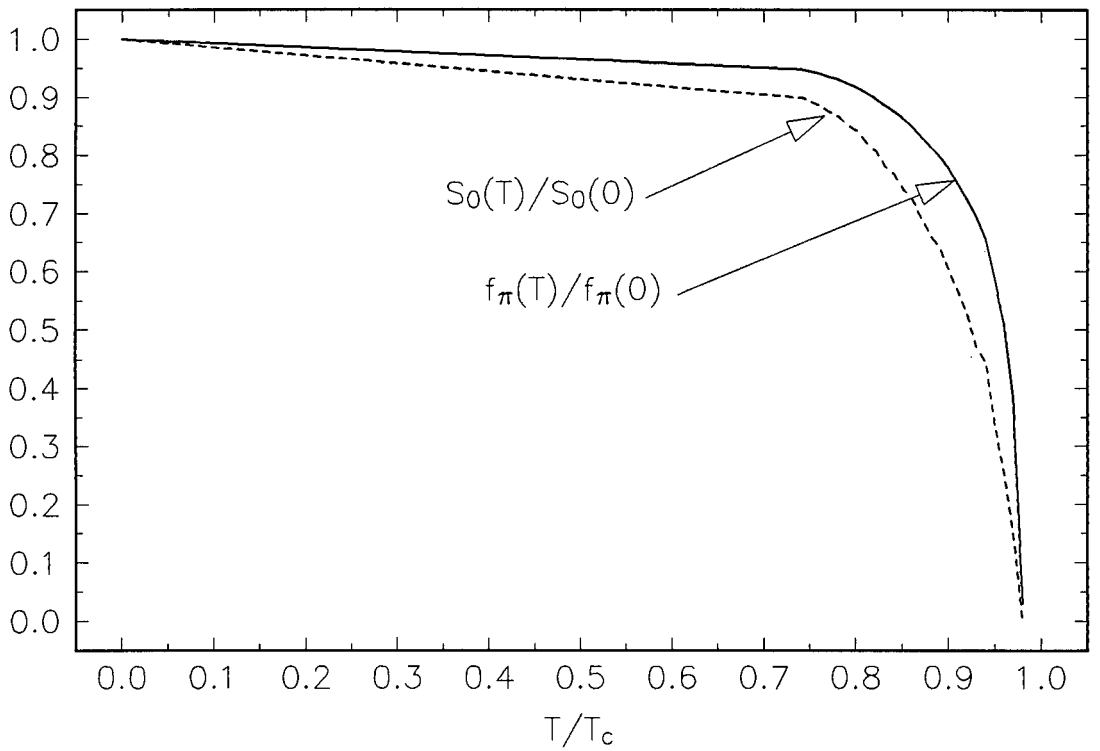

Figure 3.3: From [23] $f_\pi(T)/f_\pi(0)$ (the solid line) is graphed against T/T_d (where $T_d = 102$ MeV). From the relationship in eq.(3.59) $S_0(T)/S_0(0)$ (the dashed line) is plotted on the same system of axis.

Chapter 4

Electromagnetic pion form factor at finite temperature

In order to determine the temperature dependence of the electromagnetic pion form factor F_π [27], we will employ the results derived in chapters 2 and 3. However, unlike chapter 2 (eq.(2.1)) the basic object under investigation is the Gibb's averaged three-point function.

$$\Pi_{\mu\nu\lambda}(p,p',q,T) = i^2 \int d^4x\, d^4y\, e^{i(p'x-qy)} << T\{j^\dagger_{A\nu}(x), j^{el}_\lambda(y), j_{A\mu}(0)\} >> \qquad (4.1)$$

where $j_{A\mu}(x)$ is the axial-vector light quark current given by $j_{A\mu}(x) = \bar{u}(x)\gamma_\mu\gamma_5 d(x)$, $j^{el}_\lambda(x)$ is the electromagnetic current, and $q = p' - p$ is the momentum transfer. The Gibb's averaging $<< \cdots >>$ is defined as in eq.(3.46). As before (eq.(2.2)) the three-point function satisfies a double dispersion relation. The hadronic spectrum can be modeled by a pion pole with a hadronic continuum modeled by perturbative QCD after some threshold S_0. So similarly to eq.(2.4)

$$\begin{aligned}\rho_{\mu\nu\lambda}(s,s',Q^2,T)|_{HAD} = \; &= \; 2f_\pi^2(T)F_\pi(Q^2,T)p'_\nu p_\mu(p_\lambda + p'_\lambda)\delta(s)\delta(s') \\ &+ \; \rho_{\mu\nu\lambda}(s,s',Q^2)|_{QCD}\,[1-\theta(S_0-s-s')] \qquad (4.2)\end{aligned}$$

However here, f_π the pion decay constant, S_0 the continuum threshold and F_π depend on temperature. In the calculation that follows we will use[1] $f_\pi(T)$ and $S_0(T)$ as shown

[1]Note this calculation is performed in the chiral limit with $m_q = m_\pi = 0$

in figure 3.3. Then to set up a finite energy QCD sum rule one must calculate the finite temperature version of the lowest order loop diagram in perturbative QCD.

4.1 Calculation of the lowest order loop diagram ($T \neq 0$)

The leading order Feynman diagram in perturbative QCD for the three-point function is the one given in figure 2.1. However with non-zero temperature, the internal quark propagators in the diagram are given by eq.(3.44) (the finite temperature Fermion propagator as derived in the Dolan Jackiw formalism). Now in the chiral limit the finite temperature propagator in eq.(3.44) becomes

$$\bar{S}_\beta(k) = i \not{k} \left(\frac{1}{k^2 + i\epsilon} + i2\pi n_F(|k_0|)\delta(k^2) \right) \tag{4.3}$$

and thus

$$\Pi^{(0)}_{\mu\nu\lambda}(p, p', q, T) = \int \frac{d^4k}{(2\pi)^4} Tr\{\gamma_\nu\gamma_5 \bar{S}_\beta(k)\gamma_\mu\gamma_5 \bar{S}_\beta(p-k)\gamma_\lambda \bar{S}_\beta(p'-k)\} \tag{4.4}$$

where k, $p-k$ and $p'-k$ are the 4-momenta of the three internal quark lines. Now as in section 2.3 we want to get $\rho^{(0)}_{\mu\nu\lambda}(s, s', Q^2, T)$ and so we will obtain it by putting the quark lines on-mass-shell and employing Cutkosky's rule ($1/k^2 \to -2\pi i\delta(k^2)$). Doing this to the propagator in eq.(4.3), it becomes

$$\begin{aligned} \bar{S}_\beta(k) &= 2\pi \not{k} \delta(k^2)[1 - n_F(|k_0|)] \\ &= 2\pi \not{k} \delta(k^2) - 2\pi \not{k} n_F(|k_0|)\delta(k^2) \end{aligned} \tag{4.5}$$

So the temperature dependent quark propagator can be written as the sum of two propagators. The first being the zero temperature quark propagator and the second is the zero temperature quark propagator with a thermal insertion of a Fermi-factor of $-n_F(|k_0|)$. In the three-point function (eq.(4.4)) we have the product of three finite temperature quark propagators. So if we expand this product we get eight momentum integrals. The first is the integral with three zero-temperature quark propagators, three are with one thermal insertion along each internal leg, three are with two thermal insertions along internal legs

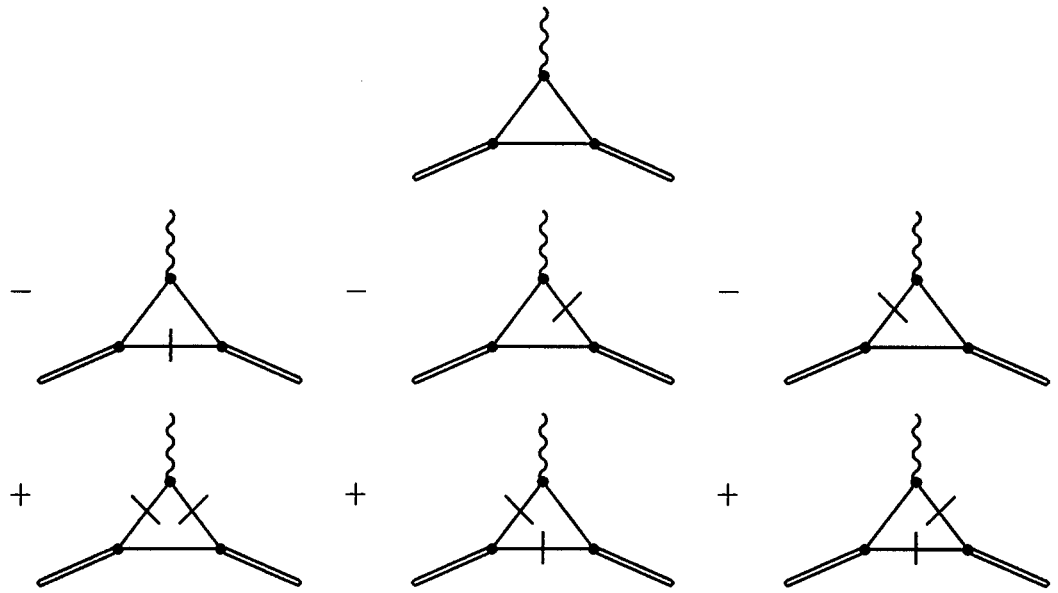

Figure 4.1: Here we can see the seven first order loop diagrams contributing to the QCD spectral function. In the diagrams a straight internal quark line indicates a zero temperature propagator ($2\pi \not{k}\delta(k^2)$) and a line with a slash through it indicates a zero temperature quark propagator with a thermal insertion ($-2\pi \not{k}\delta(k^2)n_F(|k_0|)$).

and the last with three thermal insertions. The last integral (with three thermal insertions) does not contribute to the spectral function as it is real and thus has no imaginary part ($\rho_{\mu\nu\lambda} = Im\,\Pi_{\mu\nu\lambda}$). So the seven remaining integrals can be seen in figure 4.1.

The first graph in figure 4.1 is exactly the same as the graph evaluated earlier in the zero temperature case. So in order to determine the finite temperature QCD spectral function we need to be able to evaluate the Feynman diagrams with thermal insertions. I will evaluate one of the diagrams and it will become self-evident how the other evaluations can be done. So a typical integral with one thermal insertion is (this corresponds to the left most loop diagram on the second line of figure 4.1)

$$-\int d^4k\, k_\mu (p-k)_\nu (p'-k)_\lambda \delta[k^2]\delta[(p-k)^2]\delta[(p'-k)^2] n_F(|k_0|) \qquad (4.6)$$

We will soon see that evaluation of the integral in eq.(4.6) will yield the $T = 0$ result

multiplied by a thermal factor. As before in chapter 2 this integral can be split into four intrinsic integrals I, I_μ, $I_{\mu\nu}$ and $I_{\mu\nu\lambda}$. But as we observed before the integrals I_μ, $I_{\mu\nu}$ and $I_{\mu\nu\lambda}$ are just some tensor structures multiplied by the result of the integral I. So evaluation of the integral I will show the additional thermal factor.

$$I = \int d^4k\, \delta[k^2]\delta[(p-k)^2]\delta[(p'-k)^2] n_F(|k_0|) \tag{4.7}$$

So we can proceed to evaluate this integral as before, stopping prior to the final step, as in eq.(2.16), then

$$\begin{aligned} I &= \frac{\pi}{4\,|p'_0|\vec{p}| + p_0|\vec{p}'||} \int dz \left\{ \delta\left[z - \frac{1}{2}\frac{p'^2|\vec{p}| + p^2|\vec{p}'|}{|p'_0|\vec{p}| + p_0|\vec{p}'||} \right] \right. \\ &\quad \left. + \delta\left[z + \frac{1}{2}\frac{p'^2|\vec{p}| + p^2|\vec{p}'|}{|p'_0|\vec{p}| + p_0|\vec{p}'||} \right] \right\} n_F(|z|) \end{aligned} \tag{4.8}$$

remembering the substitution $z = |\vec{k}| = k_0$. Before, without the thermal insertion (eq.(2.16)) the integral on the right of eq.(4.8) yielded unity, however now this integral with the δ-functions will yield the thermal factor. Up to now this evaluation has been performed in reasonable generality, but we will now choose a particular reference frame where $p_\mu = (p_0, \vec{0})$ and $p'_\mu = (p'_0, \vec{p}')$ (i.e. we are in a frame at rest with respect to the pion heat bath). Then the δ-functions in the integral become $\delta[z \pm \frac{1}{2}\sqrt{\frac{x+y}{2}}]$ (remember $p_0 = \sqrt{p^2} = \sqrt{s} = \sqrt{\frac{x+y}{2}}$]). Then in this frame the integral I (eq.(4.8)) becomes (with λ defined as before in eq.(2.19))

$$I = \frac{\pi}{2\lambda^{1/2}} n_F\left(\left| \frac{1}{2}\sqrt{\frac{x+y}{2}} \right| \right) \tag{4.9}$$

Similarly I_μ, $I_{\mu\nu}$ and $I_{\mu\nu\lambda}$ are now the product of their previous values (their zero temperature values) multiplied by a common thermal factor ($n_F(|\frac{1}{2}\sqrt{\frac{x+y}{2}}|)$). Thus the loop diagram with one thermal insertion (eq.(4.6)) yields the following contribution to the temp dependent QCD spectral function.

$$-\rho^{(0)}_{\mu\nu\lambda}(s, s', Q^2) n_F\left(\left| \frac{1}{2}\sqrt{\frac{x+y}{2}} \right| \right) \tag{4.10}$$

where $\rho^{(0)}_{\mu\nu\lambda}(s, s', Q^2)$ is the zero temperature spectral function in eq.(2.24).

Similarly the other loop diagrams will contribute the same zero temperature spectral function multiplied by a thermal factor comprising of either one or two Fermi-factors and a negative or positive sign (depending on whether the diagram had one or two thermal insertions). Thus the temperature dependent spectral function for the first order loop in perturbative QCD is

$$\rho_{\mu\nu\lambda}(s,s',Q^2,T)|_{QCD} = \rho^{(0)}_{\mu\nu\lambda}(s,s',Q^2)|_{QCD}\{1-n_1-n_2-n_3+n_1n_2+n_1n_3+n_2n_3\} \tag{4.11}$$

where

$$n_1 = n_2 \equiv n_F\left(\left|\frac{1}{2}\sqrt{\frac{x+y}{2}}\right|\right) \tag{4.12}$$

$$n_3 \equiv n_F\left(\left|\frac{Q^2+(x-y)/2}{2\sqrt{\frac{x+y}{2}}}\right|\right) \tag{4.13}$$

where the temperature dependence is buried in the definition of the Fermi-factors. The factors n_1 and n_2 come from the thermal insertions $n_F(|k_0|)$ and $n_F(|p_0-k_0|)$ and the n_3 arises from the insertion of $n_F(|p'_0-k_0|)$ ($p'_0-k_0 = \frac{x+Q^2}{2\sqrt{\frac{x+y}{2}}} - \frac{1}{2}\sqrt{\frac{x+y}{2}} = \frac{Q^2+(x-y)/2}{\sqrt{2(x+y)}}$ comes from the choice of reference frame $p_\mu = (p_0,\vec{0})$ and $p'_\mu = (p'_0,\vec{p}')$).

Unlike in the calculation in section 3.3 of the two-point function, here we only have graphs in the time-like region. Space-like scattering Feynman diagrams do not contribute to the spectral function. This is because the three-point function has three external momentum legs and thus one does not have to take the three-momentum to zero in order to compute the diagram unlike the two-point function (in the case of the two-point function one needs to let $\vec{p} \to 0$ in order for the cut centered about $\omega = 0$ to become a δ-function of ω^2).

4.2 The finite temperature sum rule for F_π

Thus similarly to eq.(2.30) we obtain the following finite energy QCD sum rule.

$$F_\pi(Q^2,T) = \frac{1}{f_\pi^2(T)}\int_0^{S_0(T)} dx \int_{-x}^{x} dy\, \rho(x,y,Q^2)|_{QCD} F(x,y,Q^2,T) \tag{4.14}$$

where

$$F(x,y,Q^2,T) = 1 - n_1 - n_2 - n_3 + n_1n_2 + n_1n_3 + n_2n_3 \tag{4.15}$$

and n_1, n_2 and n_3 are as defined in eq's (4.12) and (4.13). The $\rho(x,y,Q^2)|_{QCD}$ is the coefficient of the tensor structure $P_\mu P_\nu P_\lambda$ (see eq.(2.27)) in the zero temperature case.

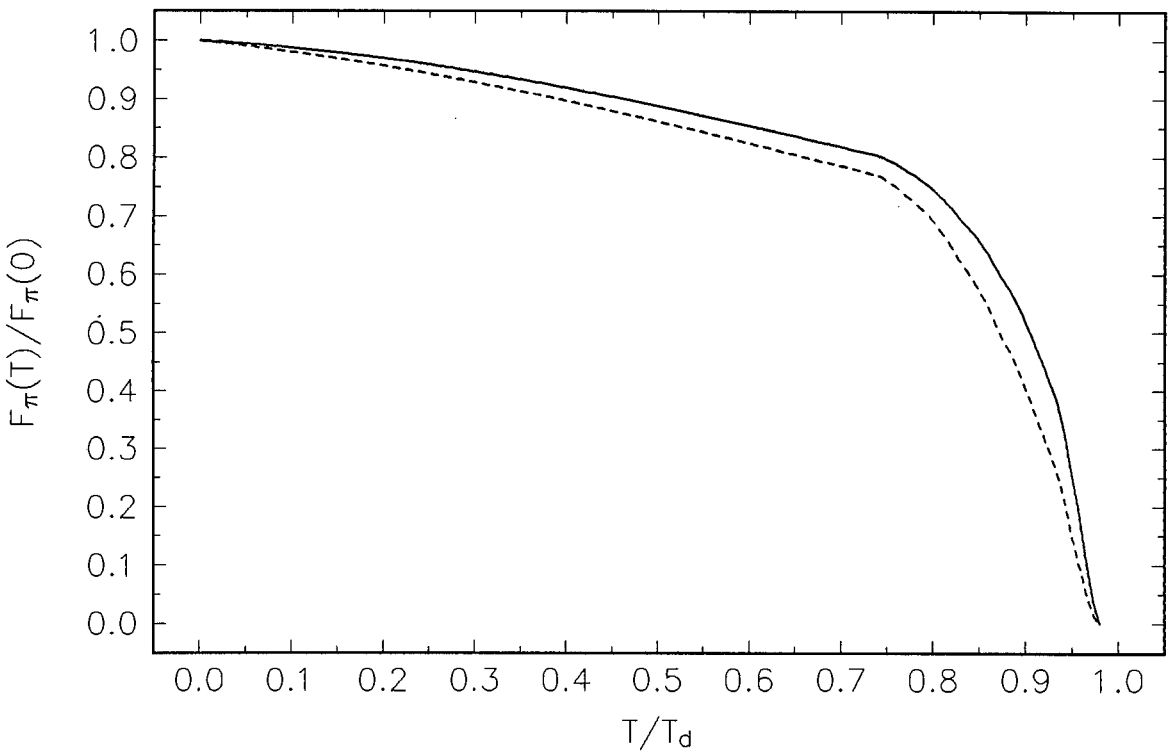

Figure 4.2: Plot of $F_\pi(Q^2,T)/F_\pi(Q^2,0)$ against T/T_d (T_d = 102 MeV) for Q^2 = 1 GeV^2 (solid curve) and Q^2 = 3 GeV^2 (dashed curve).

Unlike in the zero temperature case this expression eq.(4.14) is not exactly analytically solvable. However it can be computed numerically. For the numerical calculation I have used the values for $f_\pi(T)$ from [23] and for $S_0(T)$ from the relationship in eq.(3.59) (a graph of the ratios $f_\pi(T)/f_\pi(0)$ and $S_0(T)/S_0(0)$ can be seen in figure 3.3). In order to perform the numerical two-dimensional integration I have used a numerical 20 point Gaussian integration routine over each dimension (positions and weights for the Gaussian integral come from Abramowitz and Stegun [28]). A plot of $F_\pi(Q^2,T)/F_\pi(Q^2,0)$ against T/T_d (T_d = 102 MeV) can be seen in figure 4.2 with Q^2 = 1 GeV^2 (solid curve) and

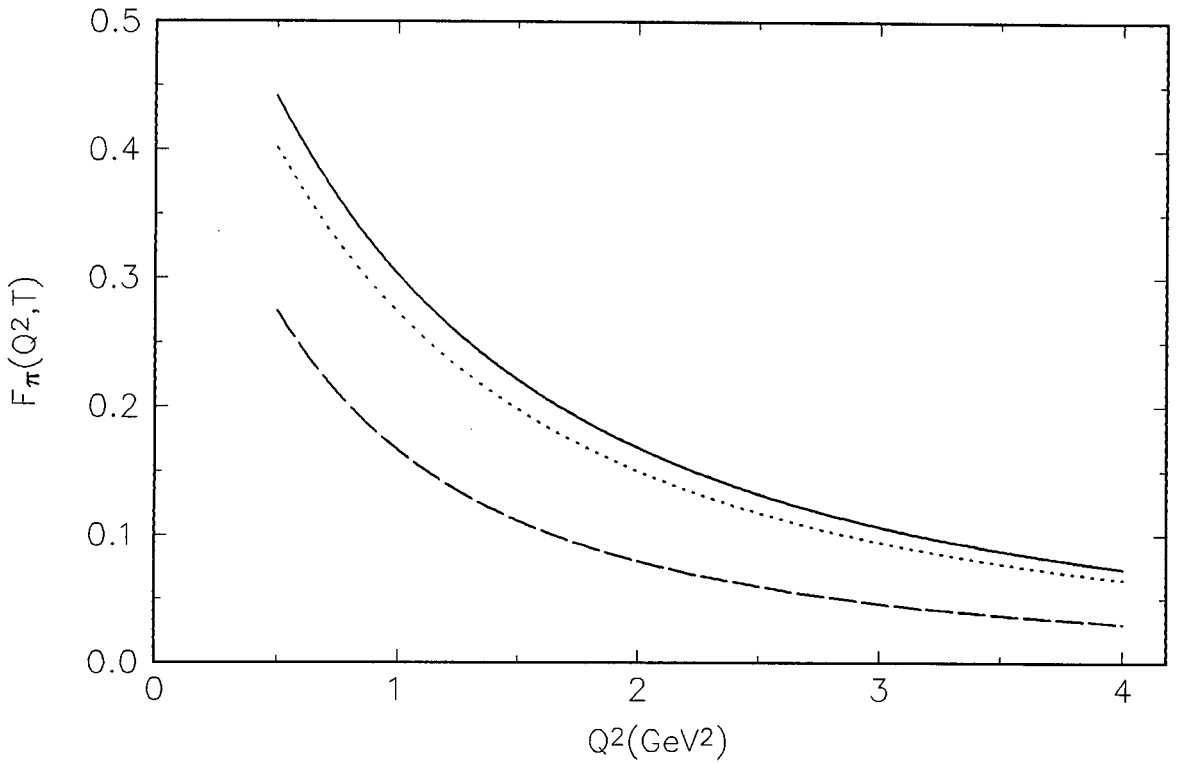

Figure 4.3: Plot of $F_\pi(Q^2,T)$ against Q^2 for $T/T_d = 0.3$ (solid curve), $T/T_d = 0.6$ (dotted curve), $T/T_d = 0.9$ (dashed curve).

$Q^2 = 3$ GeV^2 (dashed curve). A plot of $F_\pi(Q^2,T)$ against Q^2 for Q^2 between 0.5 and 4 GeV^2 can be seen in figure 4.3 for the following temperatures: $T/T_d = 0.3$ (solid curve), $T/T_d = 0.6$ (dotted curve), $T/T_d = 0.9$ (dashed curve). The result for $F_\pi(Q^2,T)/F_\pi(Q^2,0)$ in figure 4.2 is consistent with the expectation that as the temperature increases F_π should decrease and vanish at the critical temperature for deconfinement (T_d). Also in figure 4.3 we see that as the temperature approaches the critical temperature, the form factor F_π vanishes.

This result is essentially independent of the choice of reference frame. For instance, one could choose a frame where $p_\mu = (p_0, \vec{p})$ and $p'_\mu = (p'_0, -\vec{p})$, which leads to different arguments in the thermal factors, but roughly the same graph of $F_\pi(Q^2,T)/F_\pi(Q^2,0)$.

4.3 Estimate of the temperature dependence of the mean-square pion radius $< r_\pi^2 >_T$

Although the OPE breaks down at small values of Q^2 one may still extrapolate with our expression for $F_\pi(Q^2,T)$ (eq.(4.14)) into this region in order to study the qualitative behaviour of the mean-square-radius $< r_\pi^2 >_T$ / $< r_\pi^2 >_0$. The definition of $< r_\pi^2 >_T$ is as follows

$$< r_\pi^2 >_T = \frac{6}{F_\pi(0,T)} \frac{\partial F_\pi(Q^2,T)}{\partial Q^2}\bigg|_{Q^2=0} \tag{4.16}$$

So in order to determine $< r_\pi^2 >_T$ one needs an estimate of $\partial F_\pi(Q^2,T)/\partial Q^2|_{Q^2=0}$. This can be done by taking the derivative of eq.(4.14) with respect to Q^2 and letting $Q^2 \rightarrow 0$. Thus one needs the derivative of the spectral function in eq.(4.14) with respect to Q^2. Now the spectral function is

$$\rho(x,y,Q^2,T)|_{QCD} = \rho(x,y,Q^2)|_{QCD} F(x,y,Q^2,T) \tag{4.17}$$

so then

$$\frac{\partial \rho(x,y,Q^2,T)|_{QCD}}{\partial Q^2} = \frac{\partial \rho(x,y,Q^2)|_{QCD}}{\partial Q^2} F + \rho(x,y,Q^2)|_{QCD} \frac{\partial F}{\partial Q^2} \tag{4.18}$$

and

$$\frac{\partial F}{\partial Q^2} = \frac{n_3(n_3-1)(2n_1-1)}{\sqrt{2(x+y)}} \tag{4.19}$$

where F is defined as in eq.(4.15) and n_1, n_3 are defined as in eq's (4.12) and (4.13) respectively. $\partial \rho(x,y,Q^2)|_{QCD}/\partial Q^2$ can be calculated from the expression for $\rho(x,y,Q^2)|_{QCD}$ using a computer program like DERIVE or MATHEMATICA. So we can use numerical integration (a 20 point Gaussian integration routine along the x-axis and a 60 point Gaussian integration routine along the y-axis) to calculate $\partial F_\pi(Q^2,T)/\partial Q^2$. We then let $Q^2 \rightarrow 0$. Due to the numerics I was unable to take Q^2 right to zero, but for a small value of Q^2 one obtains the graph of $< r_\pi^2 >_T$ / $< r_\pi^2 >_0$.

In figure 4.4 we can see that this ratio increases monotonically with T, doubling at $T/T_d \simeq 0.8$ and diverging at the critical temperature. The divergence of $< r_\pi^2 >_T$

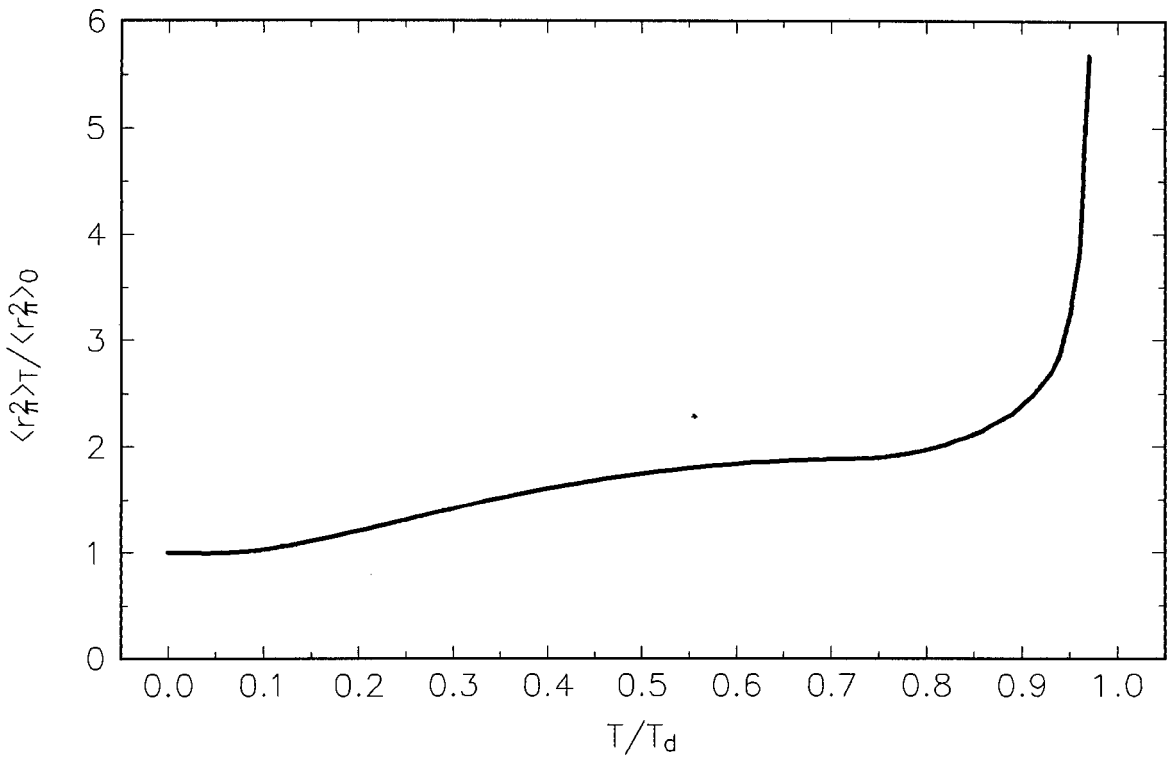

Figure 4.4: Plot of $< r_\pi^2 >_T$ / $< r_\pi^2 >_0$ against T/T_d.

may be interpreted as a signal for quark deconfinement. The behaviour of $< r_\pi^2 >_T$ can be traced to the temperature behaviour of $S_0(T)$. As $S_0(T)$ decreases with increasing T, the mean-square-radius increases. This is in qualitative agreement with that obtained in the framework of the Nambu-Jona Lasinio model [29].

4.4 Conclusion

In the second chapter a zero temperature calculation for the electromagnetic pion form factor $F_\pi(Q^2)$ was presented, following [12]-[14]. This showed the characteristic behaviour of F_π with respect to Q^2, the 4-momentum transfer. In figure 2.4 we can see that F_π decreases with increasing Q^2.

In the third chapter we first saw how the quark and gluon propagators can be modified to

be temperature dependent. This was done using the Dolan-Jackiw formalism. The finite temperature QCD sum rules formalism was then introduced (based on the initial work of Bochkarev and Shaposhnikov [20]). Using this formalism a finite temperature (Gibb's averaged) two-point function associated with the axial-vector current was considered. This calculation (as performed by [21]) yielded the temperature dependence of the continuum threshold $S_0(T)$ (one also needs $f_\pi(T)$ which comes from [23]).

With the knowledge of the finite temperature QCD sum rules formalism and the temperature dependence of the quark propagator, I was able to perform the finite temperature calculation of the first order loop diagram in perturbative QCD corresponding to the three-point function. Then much like in the zero temperature case (in chapter 2) one can setup a sum rule for the finite temperature form factor $F_\pi(Q^2, T)$. Thus $F_\pi(Q^2, T)$ can be computed numerically with the knowledge of $S_0(T)$ and $f_\pi(T)$ from chapter 3. As can be seen in figures 4.2 and 4.3 as the temperature approaches the critical temperature for deconfinement $F_\pi(Q^2, T)$ vanishes. This is consistent with our expectation that for temperatures exceeding the critical temperature the pion would cease to exist. Also the qualitative evaluation of the mean-square pion radius (see figure 4.4) shows the radius diverging as the temperature approaches the deconfinement phase transition.

Acknowledgements

- The work presented here is due, in a large part, to the patient understanding and encouragement of my supervisor, Prof. C.A. Dominguez. His assistance is greatly appreciated.

- I also wish to thank my family, and those friends and fellow physicists who have encouraged me to enjoy physics and life to the full.

- This work has been partially supported by the FRD and UCT in the form of post-graduate scholarships and awards, my thanks go to them for their generous support.

Appendix A

The Borel transform

If one has a function $f(r)$ such that

$$f(r) = \frac{1}{\pi}\int_0^\infty ds\,\frac{Im\,f(s)}{s+r} \tag{A.1}$$

then the Borel transform of $f(r)$ is

$$f(M^2) \equiv \mathcal{B}_{M^2} f(r) = \lim_{\substack{n\to\infty \\ r\to\infty \\ r/n\to M^2}} \frac{r^{n+1}}{n!}\left(-\frac{d}{dr}\right)^n f(r) \tag{A.2}$$

$$= \frac{1}{\pi}\int_0^\infty ds\, e^{-s/M^2} Im\, f(s) \tag{A.3}$$

Thus a double Borel transform of a function (spectral function) $f(r, r', Q^2)$ is

$$\mathcal{B}_{M^2}\mathcal{B}'_{M^2} f(r, r', Q^2) = \int_0^\infty ds \int_0^\infty ds'\, e^{-(s+s')/M^2} Im\, f(s, s', Q^2) \tag{A.4}$$

Q^2 being an independant variable. In our case $\rho(s, s', Q^2) = Im\, f(s, s', Q^2)$.

Bibliography

[1] M. Gell-Mann, Phys. Lett. **8** (1964) 214.

[2] F. Halzen and A.D. Martin, **Quarks & Leptons: An Intoductory Course in Modern Particle Physics**, Wiley, Singapore, 1984.

[3] E. de Rafael, **Quantum Chromodynamics as a Theoretical Framework of the Hadronic Interactions**, Ecole d'Eté de Physique des Particules, Gif-sur-Yvette, 1978; Springer L.N.P. 118 (1980).

[4] T. Sloan, G. Smadja and R. Voss, Phys. Rep. **162** (1988) 45.

[5] S.L. Wu, Phys. Rep. **107** (1984) 59.

[6] H.D. Politzer, Phys. Rev. Lett. **30** (1973) 1346.

[7] D.J. Gross and F. Wilczek, Phys. Rev. **D8** (1973) 3633.

[8] M.A. Shifman, A.I. Vainshtein and V.I. Zakharov, Nucl. Phys. **B147** (1979) 385, 448.

[9] K. Wilson, Phys. Rev. **179** (1969) 1499.

[10] L.J. Reinders, H. Rubinstein and S. Yazaki, Phys. Rep. **C127** (1985) 1; L.J. Reinders, H.R. Rubenstein, S. Yazaki, Nucl. Phys. **B197** (1982) 55.

[11] B.L. Ioffe, Nucl. Phys. **B188** (1981) 817; (E: **B191** (1981) 591).

[12] B.L. Ioffe and A.V. Smilga, Nucl. Phys. **B216** (1983) 373.

[13] V.A. Nesterenko and A.V. Radyushkin, Phys. Lett. **B115** (1982) 410.

[14] V.L. Eletsky and Ya.I. Kogan, Z. Phys. **C20** (1983) 357.

[15] K.G. Chetyrkin, S.G. Gorishny, A.B. Krasulin, S.A. Larin, V.A. Matveev, (Moscow INR) **IYaI-P-0337** (1984).

[16] K.G. Chetyrkin, A.B. Krasulin, V.A. Matveev, JETP Lett. **41** (1985) 272.

[17] H. Pietschmann, **Weak Interactions–Formulae, Results, and Derivations.** Springer Verlag, Wien-New York, 1974.

[18] C. Debek et al., Phys. Rev. **D17** (1978) 1793.

[19] L. Dolan and R. Jackiw, Phys. Rev. **D9** (1974) 3320.

[20] A.I. Bochkarev and M.E. Shaposhnikov, Nucl. Phys. **B268** (1986) 220.

[21] C.A. Dominguez and M. Loewe, Phys. Lett. **B233** (1989) 201.

[22] C.A. Dominguez and M. Loewe, Z. Phys. **C58** (1993) 273.

[23] A. Barducci, R. Casalbuoni, S. de Curtis, R. Gatto, and G. Pettini, Phys. Lett. **B244** (1990) 311.

[24] V.A. Novikov, M.A. Shifman, A.I. Vainshtein and V.I.Zakharov, Phys. Rep. **C116** (1984) 103 ; Nucl. Phys. **B249** (1985) 445.

[25] C.A. Dominguez and M. Loewe, University of Cape Town Report No. **UCT-TP-208/94** (1994).

[26] J. Gasser and H. Leutwyler, Phys. Lett. **B184** (1987) 83.

[27] C.A. Dominguez, M. Loewe, J.S. Rozowsky, University of Cape Town Report No. **UCT-TP-215/94** (1994).

[28] M. Abramowitz and I.A. Stegun, **Pocketbook of Mathematical Functions.** Verlag Harri Deutsch, Thun-Frankfurt/Main, 1984.

[29] H-J. Schulze, J. Phys. **G20** (1994) 531.